

## **Supporting online material**

### **Materials and Methods**

#### *Yeast strains*

All yeast strains were derived from an S288C *lys1Δ::kanMX; arg4Δ::kanMX* parent (a generous gift of Ole Jensen, University of Southern Denmark). Additional strains were *cdc28Δ::cdc28-as1* (LH152) and *cdc28Δ::cdc28-as1; Clb2-HA::GAL-Clb2-ΔN-URA3* (LH518).

#### *Yeast culture conditions*

We used the analog-sensitive *cdk1-as1* strain, in which the endogenous copy of the *CDK1* gene is replaced with a gene encoding a point mutant (F88G) that expands the ATP binding site of the kinase, rendering the mutant Cdk1-as1 enzyme uniquely sensitive to the bulky inhibitor 1-NM-PP1 (1). This strain allows rapid chemical inhibition of Cdk1-as1 *in vivo*. Proteins that are dynamically regulated by phosphorylation by Cdk1 and dephosphorylation by competing phosphatases (e.g. Cdc14 and PP2A) will be rapidly dephosphorylated following kinase inhibition.

To allow quantitative mass spectrometry, it is necessary to compare chemically identical phosphopeptides from two different conditions. To achieve this, we used cells of an *arg4Δ; lys1Δ* background that rely upon arginine and lysine supplied from the medium (2). We then supplied either unlabeled lysine and arginine to the “light” culture or lysine and arginine in which every carbon and nitrogen is a heavy isotope to the “heavy” culture (heavy-labeled amino acids L-Lysine·2HCl (U-<sup>13</sup>C<sub>6</sub>, 98%; U-<sup>15</sup>N<sub>2</sub>, 98%) and L-Arginine·HCl (U-<sup>13</sup>C<sub>6</sub>, 98%; U-<sup>15</sup>N<sub>4</sub>, 98%) were obtained from Cambridge Isotope Laboratories, Inc.). After 18 h, cell populations had undergone 9-12 doublings, and the heavy culture had incorporated almost 100% heavy arginine and lysine. The heavy culture was then treated for 15 min with 10 μM 1-NM-PP1 to inhibit Cdk1-as1.

Three different experiments were performed, to maximize the number of Cdk1 substrates detected and increase confidence in our site identification. First, we used asynchronous log-phase cultures. Second, cells were treated with nocodazole for 3 h to produce a metaphase arrest with high Cdk1 activity, resulting in larger numbers of Cdk1-

dependent phosphorylation events. However, one of the major Cdk1-opposing phosphatases (Cdc14) is thought to be inactive in these cells (3, 4). Since this experiment depends upon the activity of counteracting phosphatases, we performed a third experiment in which cells were arrested in late mitosis by expression of a non-degradable truncated cyclin (Clb2- $\Delta$ 2-176) from the *GAL1* promoter. In this arrest, Cdk1 activity is high and Cdc14 is at least partially active (3, 4). This approach yielded even more phosphorylation sites that decreased in concentration after Cdk1 inhibition. About 40% of the Cdk1-dependent phosphorylation sites from the third experiment were also detected in at least one of the other experiments; in 90% of these cases, these phosphopeptides decreased in abundance after Cdk1 inhibition in at least two experiments (Database S2).

#### *Preparation of peptides*

Phosphopeptide preparation and analysis were based on previous methods (5-7). Cultures were harvested by centrifugation (4000 rpm, 5 min, 4°C), and the heavy- and light-labeled cells were mixed together prior to lysing in denaturing conditions by bead-beating at 4°C (4 cycles of 90 s, with 60 s breaks in between) in a buffer containing 50 mM Tris pH 8.2, 8 M urea, 75 mM NaCl, 50 mM NaF, 50 mM  $\beta$ -glycerophosphate, 1 mM sodium orthovanadate, 10 mM sodium pyrophosphate and one protease inhibitor cocktail tablet (complete mini, EDTA-free, Roche) per 10 ml. The protein extract was then separated from the beads and insoluble material.

The protein concentration in the lysate was determined by BCA protein assay (Pierce) and ten milligrams of protein were subjected to disulfide reduction with 5 mM DTT (56°C, 25 min) and alkylation with 15 mM iodoacetamide (room temperature, 30 min in the dark). Excess iodoacetamide was captured with 5 mM DTT (room temperature, 15 min in the dark).

The denatured protein extract was then digested with 5 ng/ $\mu$ l trypsin in 25 mM Tris pH 8.2, 1 mM CaCl<sub>2</sub>, 1.5 M urea, at 37°C for 15 h to yield a tryptic lysate. Because trypsin cleaves after arginine or lysine, heavy and light versions of every peptide (except the very C-terminal peptide of each protein) should be distinguishable based upon the mass difference between the heavy and light versions of at least one lysine or arginine.

### *Phosphopeptide enrichment*

Peptide mixtures were acidified by addition of 10% TFA to a final concentration of 0.4%, clarified by centrifugation and desalted in a 500 mg tC<sub>18</sub> SepPak cartridge (Waters). Peptides were then separated into 12 fractions by SCX chromatography on a Polysulfoethyl Aspartimide (PolyLC) semi-preparative column as described (7). Each fraction was then enriched for phosphopeptides by Immobilized Metal Ion Affinity Chromatography (IMAC). Desalted peptides were dissolved in 120 µl of IMAC binding buffer (40% ACN, 25 mM FA) and incubated for 60 min with 10 µl PhosSelect IMAC resin (Sigma, St. Louis, MO) that had been previously equilibrated in the same buffer. The supernatant, containing non-phosphorylated peptides, was collected and dried for LC-MS/MS analysis to allow normalization of peptide quantifications (see below). The IMAC resin was then washed three times with 120 µl IMAC binding buffer and peptides were eluted with 3 x 70 µl 50 mM KH<sub>2</sub>PO<sub>4</sub> /NH<sub>3</sub> pH 10.0. Eluted peptides were acidified with FA, dried and desalting with C<sub>18</sub> Empore disks.

To increase the number of substrates, additional enrichment protocols were used for some experiments. For the asynchronous cells experiment, protein fractionation by SDS-PAGE was combined with IMAC phosphopeptide enrichment. For the nocodazole-arrested cells experiment, desalted SCX fractions were split in two and one sample was enriched by IMAC and the other by TiO<sub>2</sub> phosphopeptide enrichment. For the late mitotic arrest experiment, technical replicates were obtained by analyzing each sample twice by LC-MS/MS.

### *LC-MS/MS analysis*

Dried phosphopeptides (IMAC bound) and non-phosphorylated peptides (IMAC supernatant) were resuspended in 15 µl and 800 µl 5% ACN, 4% FA, respectively, and 1.5 µl was loaded onto a microcapillary column packed with C18 beads (Magic C18AQ, 5 µm, 200 Å, 125 µm x 18 cm) using a Famos autosampler (LC Packings). Peptides were separated by reverse-phase chromatography using an Agilent 1100 binary pump across a 60 min gradient of 7-28% ACN (in 0.125% FA) and online detected in a hybrid linear ion trap – Fourier transform ion cyclotron resonance (LTQ-FT, ThermoElectron, San Jose, CA) (asynchronous experiment) or a linear ion trap - Orbitrap (LTQ-Orbitrap, ThermoElectron, Bremen, Germany) (both mitotic arrest experiments) mass spectrometer using a data-

dependent TOP10 method. For each cycle, one full MS scan in the FT-ICR or the Orbitrap at  $1 \cdot 10^6$  AGC target was followed by 10 MS/MS in the LTQ at 5000 AGC target on the 10 most intense ions. Selected ions were excluded from further selection for 35 s. Ions with charge 1 or unassigned were also rejected. Maximum ion accumulation times were 1000 ms for full MS scan and 120 ms for MS/MS scans.

There was no significant overrepresentation in our mass spectrometry experiments of peptides predicted to come from protein loops and disordered regions (Table S4). Thus, the observed preferential distribution of phosphorylation sites in these regions is not due to bias in our detection methods.

#### *Database searches and data filtering*

RAW files were converted to the mzXML file format and imported into a relational database MySQL. Data analysis was performed using in-house software. MS/MS spectra were searched against a target-decoy *S. cerevisiae* ORF database using the Sequest algorithm (version 27, revision 12) (8), with 50 ppm precursor mass tolerance, tryptic enzyme specificity with 2 missed cleavages allowed and static modification of cysteines (+57.02146, carboxamidomethylation). Dynamic modifications were 79.96633 Da on Ser, Thr and Tyr (phosphorylation), 8.01420 Da on Lys (heavy), 10.00827 Da on Arg (heavy) and 15.99491 Da on Met (oxidation). XCorr and dCn' score cutoffs, mass deviation (in ppm) and peptide solution charge were empirically determined using decoy matches as a guide and aiming to maximize the number of peptide spectral matches while maintaining an estimated false-discovery rate (FDR) of  $\leq 1\%$ .

#### *Phosphorylation site localization*

Identified phosphopeptides (Database S1) were submitted to the A-score algorithm for precise site localization (5). Sites with A-score values greater than 13 were considered localized (at 95% confidence) and used for further analysis.

#### *Peptide quantification*

Relative quantifications of heavy-light peptide pairs were automatically performed from MS scans by peak intensity ratio at the XIC (extracted ion chromatogram) maxima using in-house Vista software (9). Roughly one third of all quantifications were discarded due to low

quality, including low signal-to-noise. Database S2 lists all peptides for which high-confidence quantification and H/L ratios were obtained.

#### *Data normalization*

Non-phosphorylated peptides were used as controls for normalizing ratio distributions due to uneven cell mixing of heavy and light populations. The phosphopeptide log(H/L) ratios were normalized for each independent experiment by subtracting the median  $\log_2(\text{H/L})$  from the corresponding non-phosphopeptide distribution. These corrected H/L ratios are shown in Database S2 and were used for all subsequent analyses.

#### *Structure prediction*

The structural environment of Cdk1-dependent phosphorylation sites was evaluated using secondary structure, domain and disorder prediction algorithms (10-14). The presence of a proline in the Cdk1 consensus site automatically causes the PsiPred algorithm to assign a loop. However, the PONDR algorithm does not have this limitation and indicates that Cdk1-dependent phosphorylation sites are preferentially localized within unstructured regions and outside of Pfam domains (binomial p-value  $< 10^{-29}$  and  $< 10^{-6}$ , respectively, Table S4).

## Supporting figures

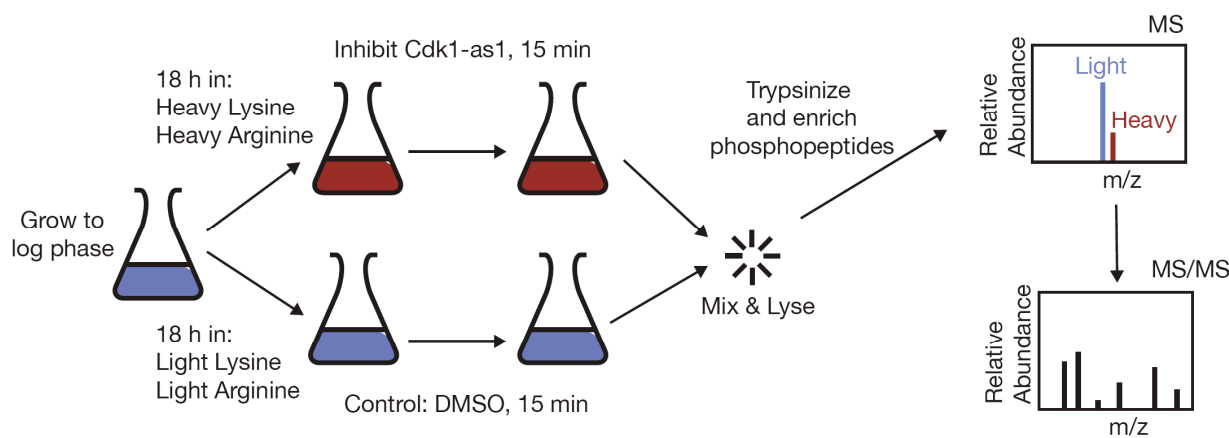
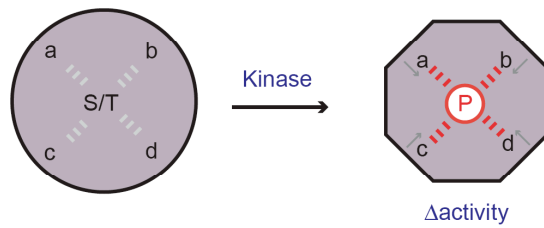


**Fig. S1.** Overview of phosphopeptide identification and relative quantification. Quantitative mass spectrometry was used to identify phosphorylation sites whose abundance decreased *in vivo* following Cdk1 inhibition. Cells of an *arg4Δ; lys1Δ* background were supplied with either regular lysine and arginine (“light” culture; blue) or lysine and arginine in which every carbon and nitrogen is a stable heavy isotope (“heavy” culture; red). 10  $\mu$ M 1-NM-PP1 was added to the heavy culture for 15 min to inhibit Cdk1. The heavy and light cultures were mixed prior to lysing in denaturing conditions. Protein extracts were then trypsinized, and phosphopeptides were purified and analyzed by tandem mass spectrometry to determine the precise amino acid sequence and sites of phosphorylation (5-7), as well as the relative abundance of the phosphopeptide in the heavy and light cultures.

A. Context-dependent



B. Plastic

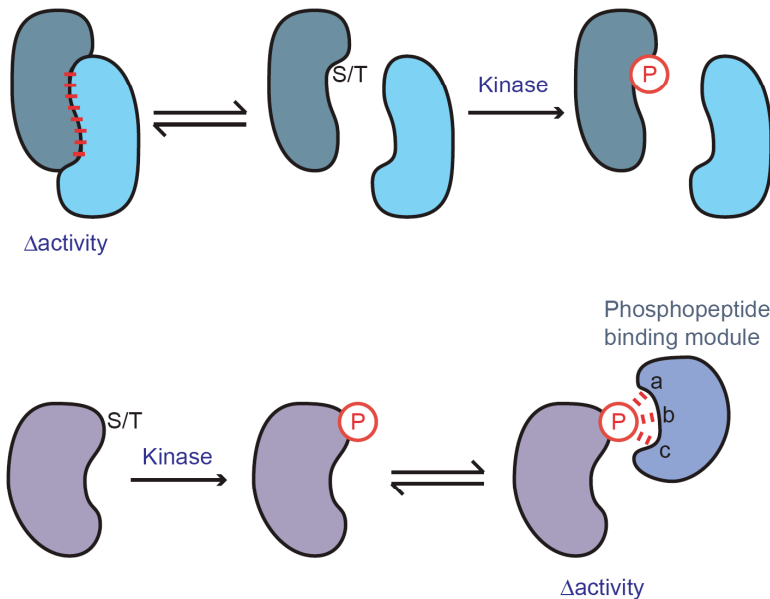


**Fig. S2.** Mechanisms of phosphoregulation. **(A)** Schematic of a form of phosphoregulation that is highly context-dependent: upon phosphorylation of a serine or threonine (S/T), a phosphate (red P) coordinates hydrogen bonds from several neighboring amino acids (a-d) to drive a precise conformational change (indicated by the change in shape from circle to octagon) and thereby alters protein activity. The precise position of the phosphate is important in this type of regulation because the phosphate needs to coordinate interactions with several amino acids. **(B)** Schematic of flexible modes of phosphoregulation. Phosphates can affect protein activity by simply preventing protein interactions (top) or by binding to modular phosphate-binding domains (bottom). This type of regulation is more plastic because similar regulation can be inferred from several positions of phosphorylation within the protein.

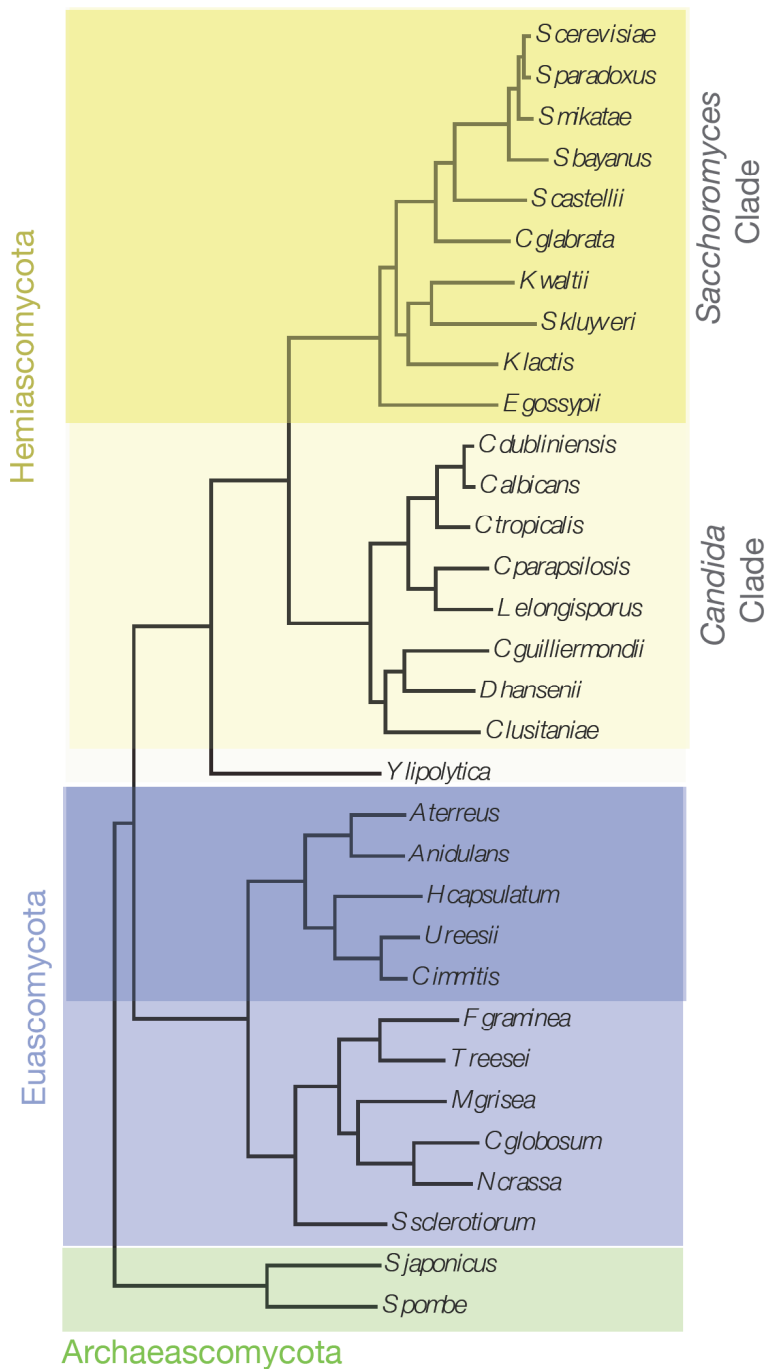


**Fig. S3.** The ascomycete phylogeny. A phylogeny describing the evolutionary relationships among 32 ascomycete species was inferred using a genomic approach (15). The major clades are distinguished by color: Hemiascomycota (yellow); Euascomycota (blue); and Archaeascomycota (green). The Hemiascomycota contain two clades that are relatively well separated in terms of their behavior in our analyses: the *Saccharomyces* clade and the *Candida* clade.

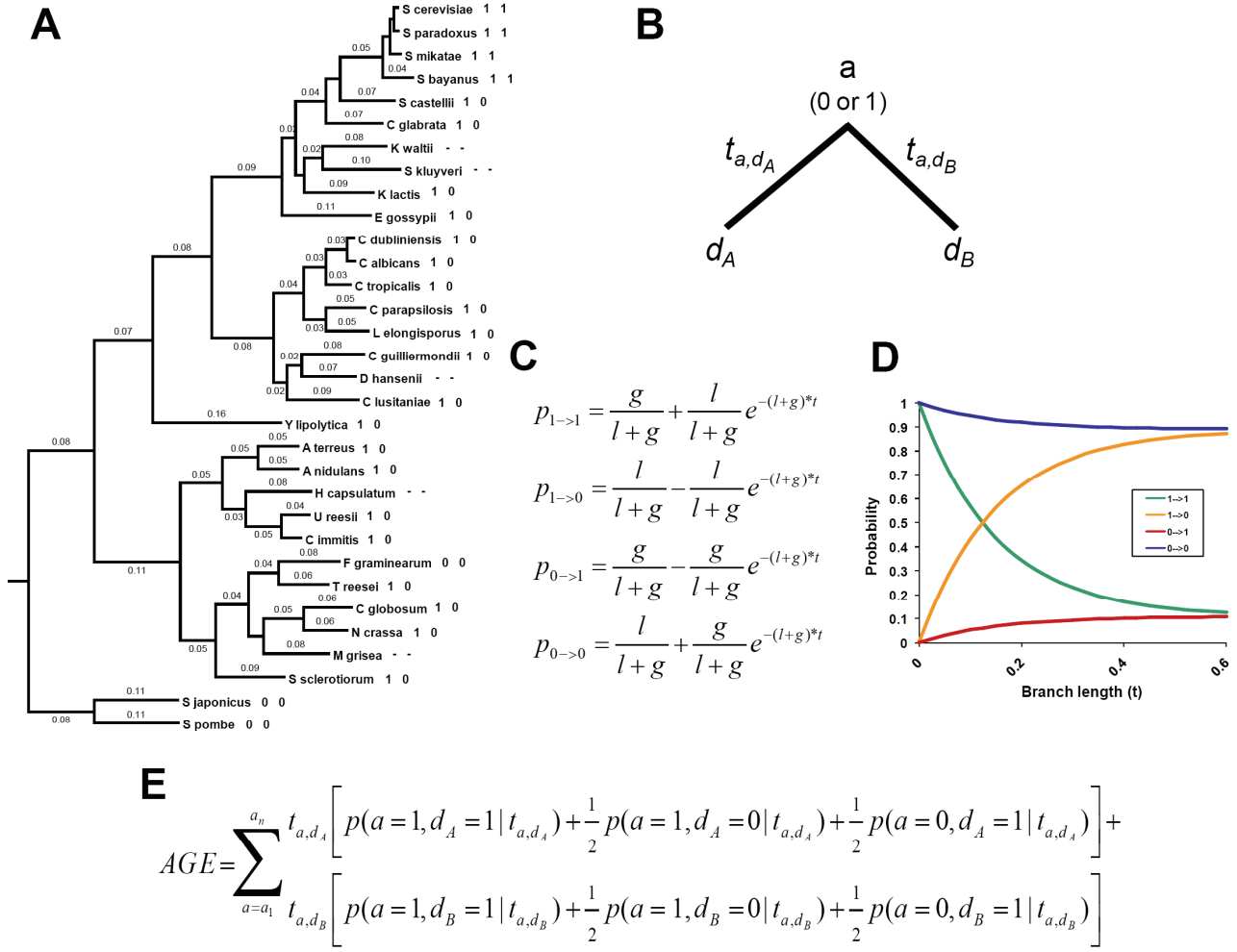


**Fig. S4.** Maximum likelihood method for inferring the “age” of a precise phosphorylation site or the “age” of enrichment of consensus sites in a protein. We inferred the “age” (i.e., level of conservation within the fungal phylogeny) of each phosphorylation site identified experimentally in *S. cerevisiae*. Our approach was to first assign presence (1) and absence (0) calls to each of the extant species nodes (i.e., the leaf nodes) based on conservation of the consensus Cdk1 site at the same position within a multiple sequence alignment of orthologous proteins. The species tree used (**A**) was inferred from concatenated alignments of orthologs and is robust to choice of inference algorithm (ML, parsimony and distance), as described elsewhere (15). The number next to each branch indicates branch length ( $t$ ) and the leaf nodes are annotated with presence/absence calls for the two phosphorylation sites of Shp1 from Fig. 4A (sites A and B, respectively). Using

a simple two-rate model of phosphorylation site gain ( $g$ ) and loss ( $l$ ), the probabilities of presence and absence at each ancestral node ( $a$ ) were calculated recursively, from the leaf nodes up (**B**). The gain and loss rates used in this analysis were inferred globally across our entire dataset by maximum likelihood. The probabilities of gain and loss (defined in **C**; e.g.,  $p_{0 \rightarrow 1}$  denotes the probability of gain along a branch) are a function of  $t$  (**D**). When  $t$  is small the probabilities of gain ( $p_{0 \rightarrow 1}$ ) and loss ( $p_{1 \rightarrow 0}$ ) are near zero and as  $t$  increases these probabilities increase, reaching their equilibrium levels as  $t$  extends past 0.5. Age is defined as the weighted sum of branch lengths over which a site was inferred to be present (**E**), where the weight is just the probability that the phosphorylation site was maintained ( $p_{1 \rightarrow 1}$ ) or half the probability that it was gained ( $p_{0 \rightarrow 1}$ ) or lost ( $p_{1 \rightarrow 0}$ ) along that branch. The example phosphorylation sites for Shp1 (shown here in panel **A** and also in Fig. 4A) have ages of 2.61 and 0.65, respectively.

The same method was used to infer the age of enrichment of consensus sites within each ORF found to be phosphorylated in our *S. cerevisiae* experiments. The difference in this case is that presence and absence calls made at the extant species nodes are based on enrichment of consensus phosphorylation motifs within each orthologous ORF (Poisson  $p < 0.01$  for presence of enrichment).

We expected that this method would help normalize for the effects of an uneven sampling of phylogeny (i.e., the fact that some branches of the tree are more densely populated by sequenced genomes than other parts). Indeed, as can be seen in Fig. 4B, the inferred ages have this desired property; for example, the four very closely related species of the *Saccharomyces sensu stricto* group do not contribute unfairly (i.e., as much as four more divergently related species do) to the age calculations.

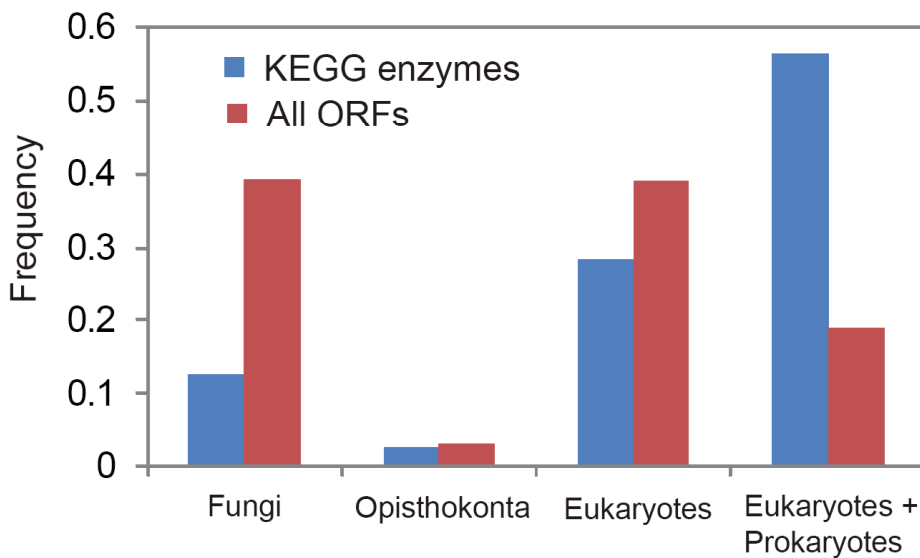
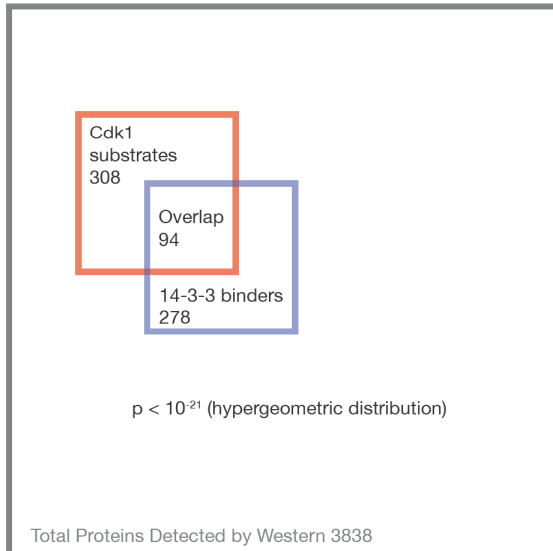


**Fig. S5.** ORFs encoding metabolic enzymes are old. The inferred ages of *S. cerevisiae* ORFs annotated as metabolic enzymes in the KEGG database (blue bars; N = 734; <http://www.genome.jp/kegg/>) were compared to the inferred ages for all ORFs in *S. cerevisiae* (red bars; N = 5480). Each ORF from *S. cerevisiae* was assigned to one of four age groups based on the most distantly related organism that was predicted to have an ortholog in the OrthoMCL ortholog mapping (16): (1) found only in fungi; (2) found only in opisthokonta (fungi and metazoa); (3) found only in eukaryotes; and (4) found in both eukaryotes and prokaryotes. More than 50% of metabolic enzymes from *S. cerevisiae* can be mapped to putative orthologs in prokaryotes, whereas this is true for less than 20% of ORFs in general. The two distributions are significantly different (Mann-Whitney  $p < 10^{-16}$ ).

A



B

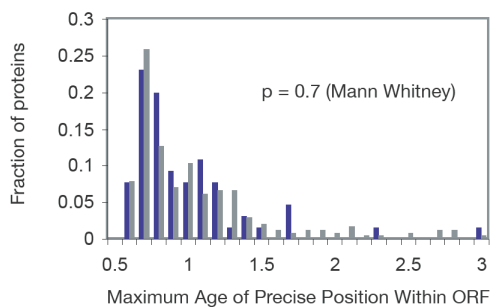
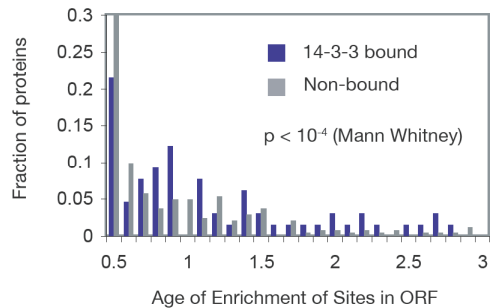


**Fig. S6.** Cdk1 targets are frequently bound by 14-3-3 proteins. **(A)** Venn diagram showing the 308 proteins that are phosphorylated by Cdk1 (red box) and the 278 proteins that were determined to interact with Bmh1 & Bmh2 in a phosphorylation-dependent manner (17) (blue box), and a conservative estimate of the total number of proteins that are present in mitotically proliferating cells (18) (gray box). Of the 278 proteins that were previously defined as 14-3-3 binding partners, 94 were targets of Cdk1. **(B)** Cdk1 target proteins that are bound by 14-3-3 proteins tend to have conservation of consensus site enrichment but not precise site position.

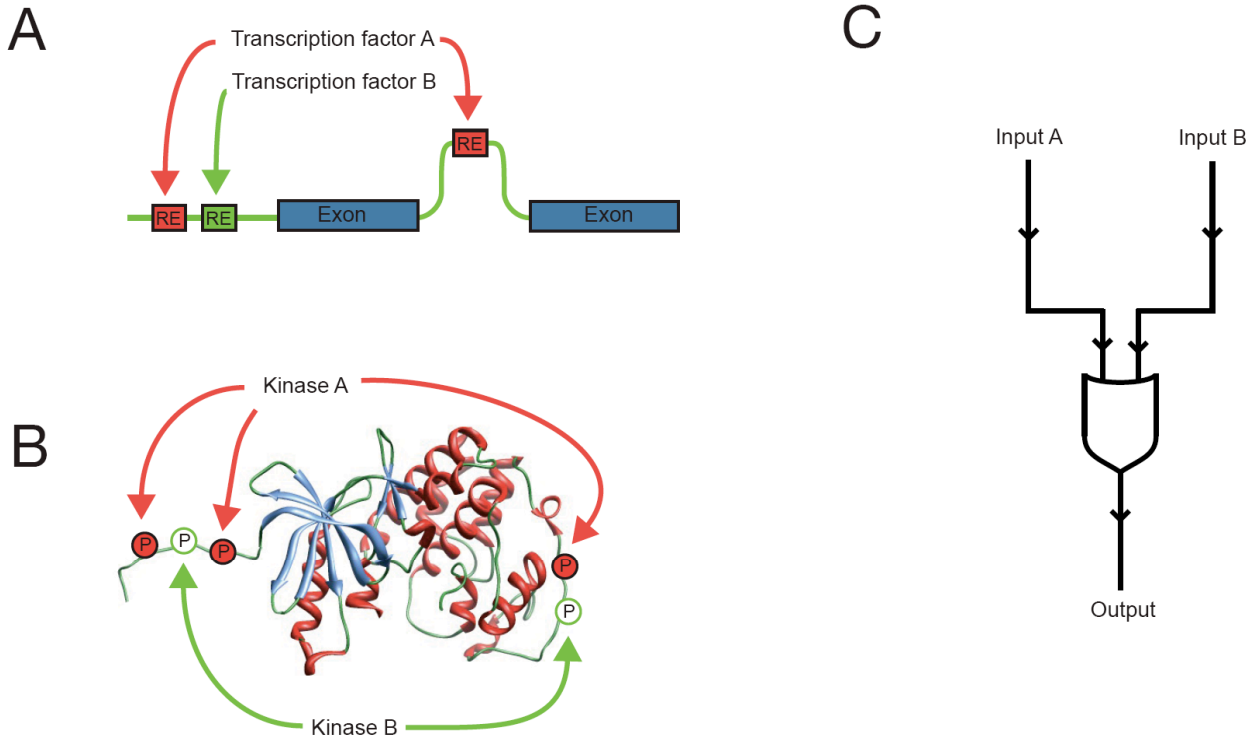


**Fig. S7.** Plasticity in transcriptional regulation and phosphoregulation. Just as simple transcriptional response elements are more likely to arise by small numbers of mutations in relatively unconstrained intergenic regions (promoters or introns, **A**), phosphorylation sites are more likely to appear in disordered regions of proteins (termini or long loops, **B**). Context-independent mechanisms of activity modulation seem to predominate in both forms of regulation, allowing for relatively easy evolution of regulation. In the example presented here, combinatorial regulation by two distinct transcription factors or kinases creates an 'OR' logic gate (**C**).

## Supporting tables

**Table S1. (Following pages)** Summary of Cdk1-dependent phosphorylation sites. This table lists the 547 phosphorylation sites that meet our criteria for identification as Cdk1 substrates (see main text): that is, they are followed by a proline and they declined in abundance by at least 50% in one or more of the three experiments. The table includes the systematic ORF name, SGD name, position of the phosphorylation site in the protein sequence (with a “#” symbol after the phosphorylation site),  $\log_2$  heavy/light (H/L) phosphopeptide abundance ratio, “age” (weighted sum of branch lengths for which regulation is predicted to be conserved) of precise site conservation and enrichment of consensus sites. Green indicates that the site is found within one of the 181 proteins previously determined to be efficiently phosphorylated by Cdk1 *in vitro* (19). This is a conservative list of peptides in which the precise position of the phosphorylation site can be inferred with high confidence (A-score greater than or equal to 13, corresponding to >95% certainty). Phosphorylation events were typically detected in several peptides, and peptides were frequently phosphorylated at multiple positions. To reduce false positives, we used the H/L ratio from peptides that only contained phosphates on Cdk1 consensus sites, or otherwise we used the peptide with the least number of phosphates. Bold font indicates the biological replicates; that is, phosphorylation sites from peptides that declined in abundance by at least 50% following Cdk1 inhibition in one experiment and also declined after Cdk1 inhibition in another experiment (these sites are also listed separately in Table S2). Database S1 contains the full list of peptides with links to MS/MS spectra, and Database S2 contains all those phosphopeptides for which H/L ratios could be determined with high confidence. There are many additional Cdk1 substrate candidates within this dataset that do not match our stringent criteria for further analysis. Note also that our method ignores Cdk1-dependent phosphorylation sites that were not rapidly dephosphorylated in any of the three conditions tested; it seems likely that additional Cdk1 targets exist among the phospho-SP and phospho-TP peptides that did not decrease in abundance following Cdk1 inhibition.

ORF	SGDB name	Site position	Context	log2 (H/L)	age precise position	age enrichment
YCR088W	ABP1	165	PPVKKSFT#PSKSPAP	-3.06	1.68	0.95
YCR088W	ABP1	169	KSFTPSKS#PAPVSKK	-3.06	0.63	0.95
YCR088W	ABP1	181	SKKEPVKT#PSPAPAA	-1.74	0.61	0.95
YCR088W	ABP1	183	KEPVKTPS#PAPAAKI	-1.32	0.63	0.95
YCR088W	ABP1	313	KGFRNEKS#PAQLWAE	-1.18	2.75	0.95
YLR131C	ACE2	486	IPGSSNNT#PIKNSLP	-3.51	1.76	2.72
YLR131C	ACE2	501	QKHVFQHT#PVKAPPK	-3.46	1.49	2.72
YLR131C	ACE2	392	SPGGLSIS#PRINGNS	-3.28	0.78	2.72
YLR131C	ACE2	385	FRLFEKTS#PGGLSIS	-3.20	0.63	2.72
YLR131C	ACE2	303	SNTSINGS#PSRKYHR	-2.64	0.90	2.72
YLR131C	ACE2	428	FTPRTQLS#PIHKKRE	-2.48	0.86	2.72
YLR131C	ACE2	259	GSPVILKT#PAMQNGR	-2.24	0.83	2.72
YLR131C	ACE2	564	SPTLHSTS#PLPDEII	-2.07	0.56	2.72
YLR131C	ACE2	80	LDIPLVPS#PKTGDGS	-1.27	0.77	2.72
YLR131C	ACE2	253	NSNSKPGS#PVILKTP	-1.06	0.78	2.72
YJR083C	ACF4	49	SKSPRVTT#PLKPKRL	-3.10	0.65	0.69
YJR083C	ACF4	62	RLAIPISS#PQRSTTN	-3.04	0.91	0.69
YJR083C	ACF4	71	QRSTTNQS#PVDHAS	-1.38	1.00	0.69
YDR216W	ADR1	188	ASSVKFQT#PTYGTPD	-2.07	0.60	0.53
YBR059C	AKL1	504	DPTISEQS#PRLNTQS	-2.86	0.60	1.40
YBR059C	AKL1	801	EALLIELS#PLKEDAG	-1.54	0.87	1.40
YJL122W	ALB1	80	TLQNASSS#PASITTR	-1.67	0.56	0.43
YOL130W	ALR1	143	YVESNIHT#PPKDVGV	-2.07	0.51	0.43
YOL130W	ALR1	188	VRKSSLVS#PVLIPH	-1.45	0.61	0.43
YKR021W	ALY1	573	VLSSPVLS#PNVQKMN	-1.42	1.19	1.48
YJL084C	ALY2	213	NGPSRNLS#PINLLKR	-2.27	1.68	1.65
YJL084C	ALY2	176	GLSSLNLN#PLGAPGN	-1.56	0.81	1.65
YKL185W	ASH1	253	TRSSKFHS#PSKESFD	-1.23	0.60	1.79
YKL185W	ASH1	452	RPKAYTPS#PRSPNYH	-1.00	1.19	1.79
YKL185W	ASH1	450	PVRPKAYT#PSPRSPN	-1.00	0.96	1.79
YKL185W	ASH1	455	AYTPSPRS#PNYHRFA	-1.00	0.88	1.79
YKL052C	ASK1	250	NSNNIESS#PLKQGHH	-2.34	1.21	0.43
YGR097W	ASK10	808	GFRSKVNT#PAIDDYG	-2.47	1.29	0.81
YDL088C	ASM4	464	SSPIVANS#PNKRLDV	-1.08	0.61	0.68
YMR068W	AVO2	315	VKTPVGVS#PKKELVS	-2.29	0.91	1.47
YBR068C	BAP2	16	SSGKKETS#PDSISIR	-1.11	0.60	0.43
YJL020C	BBC1	103	KDLPEPIS#PETKKET	-1.03	0.51	1.10
YJL095W	BCK1	816	PKPPANTS#PQRTLST	-2.73	0.83	1.95
YJL095W	BCK1	747	PKMVFKTS#PKLELNL	-1.36	0.84	1.95
YJL095W	BCK1	411	HYETNVSS#PLKQSSL	-1.33	0.89	1.95
YER167W	BCK2	418	SSMSNRYS#PIRVASP	-1.08	1.18	0.83
YIL033C	BCY1	89	RSSVMFKS#PFVNEDP	-1.19	1.71	0.43
YER155C	BEM2	1038	MLINNPAT#PNQKMRD	-1.47	0.70	1.11
YPL115C	BEM3	324	ENKALGFS#PASKEKL	-2.66	1.25	2.84
YPL115C	BEM3	254	VINNHLHS#PLKASTS	-2.50	0.91	2.84
YOR198C	BFR1	336	ADDLVLVT#PKKDDFV	-1.42	0.65	0.43
YFL007W	BLM10	11	NNDDDIKS#PIPITNK	-3.50	1.28	0.43
YFL007W	BLM10	29	QLKRFRERS#PGRPSSS	-1.95	0.76	0.43
YNL233W	BNI4	410	LRKNHDDT#PVKIDHV	-2.64	0.51	2.48
YBL085W	BOI1	540	FNRISMLS#PVKSSFD	-4.26	0.88	2.67
YBL085W	BOI1	405	PKPPSYPS#PVQPPQS	-3.02	2.23	2.67
YBL085W	BOI1	412	SPVQPPQS#PSFNNRY	-3.02	1.21	2.67
YER114C	BOI2	652	KKSSFMLS#PFRQQFT	-4.07	1.68	2.79
YER114C	BOI2	450	PKPPSYPS#PAQPPKS	-1.78	1.18	2.79
YER114C	BOI2	457	SPAQPPKS#PLLNTR	-1.78	1.05	2.79
YER114C	BOI2	519	QGGGKALS#PIPSPTR	-1.07	0.73	2.79

ORF	SGDB name	Site position	Context	log2 (H/L)	age precise position	age enrichment
YER114C	BOI2	523	KALSPIPS#PTRNSVR	-1.07	0.65	2.79
YHR036W	BRL1	56	PHFPSSPS#PLRNTLD	-2.12	1.89	1.39
YPR171W	BSP1	296	QLKPTTLS#PTMKNKP	-1.14	0.76	0.77
YPR171W	BSP1	309	KPKPTPPS#PPAKRIP	-1.10	0.63	0.77
YPR171W	BSP1	39	KPAGEALS#PVRSHNS	-1.08	0.63	0.77
YPR171W	BSP1	79	YNYEMTFS#PKKTHYS	-1.07	0.94	0.77
YKL092C	BUD2	1066	GNLGNRFS#PTKLSRI	-2.17	0.65	0.43
YCL014W	BUD3	1515	NAQKVQES#PSGPLIY	-1.86	0.75	0.90
YCL014W	BUD3	1440	PVEELPNT#PRSINVT	-1.78	0.61	0.90
YCL014W	BUD3	1549	KDEPIWVS#PSKIDFA	-1.62	1.21	0.90
YJR092W	BUD4	167	PLLSYPES#PIHRSII	-1.55	0.65	1.81
YLR319C	BUD6	327	IDDVSKAS#PLAKTPL	-1.17	0.61	0.66
YLR353W	BUD8	413	YEGHKTPS#PLTKMNK	-3.22	0.80	0.49
YLR353W	BUD8	411	SRYEGHKT#PSPLTKM	-3.22	0.63	0.49
YDL099W	BUG1	277	AARNTTAT#PIQFADF	-1.06	0.92	0.43
YKL005C	BYE1	177	DVFLDEES#PRKRKRS	-1.36	0.93	1.39
YNL278W	CAF120	556	FASSVNDS#PSDRAKS	-2.42	0.79	2.23
YNL278W	CAF120	510	SPSIKRKS#PPLVISE	-2.02	0.88	2.23
YNL278W	CAF120	518	PPLVISES#PHKVHTP	-2.02	0.70	2.23
YNL278W	CAF120	871	VQPANINS#PNKMYGA	-1.24	0.61	2.23
YNL278W	CAF120	577	NNDRKATT#PEKFERG	-1.11	0.95	2.23
YNL161W	CBK1	93	PALNYPAT#PPPNNY	-1.99	2.09	0.52
YNL161W	CBK1	109	ASNQMINT#PPPSMGG	-1.99	0.65	0.52
YFR028C	CDC14	429	SSAVPQTS#PGQPRKG	-1.42	3.07	1.45
YAL038W	CDC19	407	VLSTSTGTT#PRLVSKY	-1.89	1.23	0.43
YLR314C	CDC3	503	ELSINSAS#PNVNHSP	-2.24	0.63	0.43
YLR314C	CDC3	509	ASPVNVHS#PVPTKKK	-1.67	1.25	0.43
YMR001C	CDC5	70	KLSALCKT#PPSLIKT	-2.83	2.04	0.43
YPR019W	CDC54	69	IRAAIGSS#PLNFPSS	-1.07	2.46	0.64
YJL194W	CDC6	368	NSAQVPLT#PTTSPVK	-2.53	0.65	1.34
YJL194W	CDC6	372	VPLPTTTS#PVKKSYP	-2.53	0.65	1.34
YPL160W	CDC60	142	EEEIKEET#PAEKDHE	-1.52	0.63	0.43
YGL003C	CDH1	227	SQFFDSMS#PVRPDSK	-3.18	2.91	2.53
YBR038W	CHS2	86	YRDSAHNS#PVAPNRY	-3.58	1.08	0.43
YBR038W	CHS2	60	VFQGLPAS#PSRAALR	-2.61	1.08	0.43
YBR038W	CHS2	133	PVDPYHLS#PQQQPSN	-2.57	0.65	0.43
YBR038W	CHS2	100	YAANLQES#PKRAGEA	-1.53	1.46	0.43
YNL298W	CLA4	445	PRYAQNSS#PTAAHFQ	-1.18	0.73	1.19
YNL225C	CNM67	121	VPNFIHST#PRENSSL	-1.16	0.65	0.43
YPR030W	CSR2	963	EATSVSAS#PRSSVSY	-1.07	1.02	0.85
YOR042W	CUE5	364	AETTYIDT#PDTEKK	-1.68	1.44	0.43
YIR023W	DAL81	867	SQSSPNVT#PSHMSRH	-1.47	0.94	1.28
YGR092W	DBF2	53	AGINDSPS#PVKPSFF	-1.70	2.66	0.81
YGR092W	DBF2	51	RPAGINDS#PSPVKPS	-1.70	1.08	0.81
YGR092W	DBF2	83	PDMDVSNS#PKLPPK	-1.70	0.84	0.81
YDR052C	DBF4	11	PTKMIIRS#PLKETDT	-3.93	1.38	0.43
YHR164C	DNA2	237	KFSDLPSS#PIKAPNV	-1.57	0.65	0.73
YER088C	DOT6	487	SSDADMLS#PTHSPQK	-2.06	0.93	1.80
YER088C	DOT6	491	DMLSPTHS#PKTLSK	-2.00	0.95	1.80
YBL101C	ECM21	1028	NLDKLLST#PSPVNRS	-1.89	0.96	1.07
YBL101C	ECM21	1030	DKLLSTPS#PVNRSHN	-1.89	0.91	1.07
YBL101C	ECM21	33	KGQPFQPS#PTKKLGS	-1.58	0.65	1.07
YJL201W	ECM25	422	TPVALQNT#PVLKPKS	-1.38	0.95	0.69
YJL201W	ECM25	411	SPQRSVTS#PTYTPVA	-1.38	0.75	0.69
YBL047C	EDE1	238	VNQPNRTT#PLSANST	-1.81	0.67	1.80
YNL230C	ELA1	235	QAGGQSSS#PKGPLS	-1.03	0.61	0.43
YMR219W	ESC1	1145	DRSNIFSS#PIRVIGA	-1.69	0.63	0.43

ORF	SGDB name	Site position	Context	log2 (H/L)	age precise position	age enrichment
YBR102C	EXO84	31	AKQKTPPS#PAKPKQK	-1.82	0.92	0.43
YBR102C	EXO84	28	SSPAKQKT#PPSPAKP	-1.82	0.61	0.43
YFR019W	FAB1	183	MQNSYART#PDSDHDD	-1.15	0.70	0.49
YJL157C	FAR1	15	SFEKIKHT#PPSGDRD	-2.05	1.35	1.03
YJL157C	FAR1	8	MKT#PTRVSFE	-1.38	1.20	1.03
YDR130C	FIN1	74	VTPRIRMS#PECLKGY	-3.11	1.08	0.88
YDR130C	FIN1	36	VFVRLSMS#PLRTTSQ	-2.23	1.19	0.88
YER032W	FIR1	375	PDLEHMKS#PPSTGLN	-2.40	0.77	1.05
YER032W	FIR1	84	PNEISQDS#PLKIVFP	-2.05	0.93	1.05
YER032W	FIR1	225	NLYLTPES#PLNRYHL	-1.52	1.02	1.05
YER032W	FIR1	399	EPSEEPTS#PTRQVNP	-1.46	0.60	1.05
YNL068C	FKH2	708	GSANRARS#PLHSNSN	-1.69	1.94	2.34
YNL068C	FKH2	833	ETKDISS#PLKNQGG	<b>-1.51</b>	<b>0.60</b>	<b>2.34</b>
YPL221W	FLC1	714	SPDRASSS#PN SKSY P	-1.10	0.84	0.43
<b>YAL035W</b>	<b>FUN12</b>	<b>386</b>	<b>AKSTPAAT#PAATPTP</b>	<b>-1.07</b>	<b>0.63</b>	<b>0.43</b>
YAL034C	FUN19	211	RLP SPLAS#PNLNRQA	-2.52	0.65	1.38
YAL034C	FUN19	207	SSSSRLPS#PLASP NL	-2.52	0.65	1.38
<b>YOR178C</b>	<b>GAC1</b>	<b>66</b>	<b>KSEIFCTS#PEKNVR F</b>	<b>-1.70</b>	<b>0.64</b>	<b>1.49</b>
YOL051W	GAL11	163	QQQRQLT#PQQQQQLV	-1.24	0.74	1.37
YPL248C	GAL4	703	SPG SVGPS#PVPLKSG	-1.02	0.65	0.62
<b>YDL226C</b>	<b>GCS1</b>	<b>170</b>	<b>LENRSAT#PANSSNG</b>	<b>-4.40</b>	<b>1.11</b>	<b>0.43</b>
<b>YDL226C</b>	<b>GCS1</b>	<b>161</b>	<b>VAQSREGT#PLENRRS</b>	<b>-1.32</b>	<b>1.89</b>	<b>0.43</b>
YMR255W	GFD1	111	EISPPPVS#PSKMKTT	-1.87	0.65	0.44
YMR255W	GFD1	106	SQKATEIS#PPP VSPS	-1.43	0.60	0.44
<b>YDR309C</b>	<b>GIC2</b>	<b>337</b>	<b>AFFPSRQS#PLPKRRN</b>	<b>-3.37</b>	<b>0.79</b>	<b>0.85</b>
<b>YDR507C</b>	<b>GIN4</b>	<b>462</b>	<b>IVNQSSPT#PASRNKR</b>	<b>-3.48</b>	<b>0.65</b>	<b>0.43</b>
<b>YDR507C</b>	<b>GIN4</b>	<b>435</b>	<b>ASSNLTT#PGSSKRL</b>	<b>-2.46</b>	<b>0.76</b>	<b>0.43</b>
<b>YDR507C</b>	<b>GIN4</b>	<b>460</b>	<b>STIVNQSS#PTPASN R</b>	<b>-1.74</b>	<b>0.87</b>	<b>0.43</b>
YER054C	GIP2	213	GVQARDGS#PMLIRSK	-1.18	0.65	1.26
YAL031C	GIP4	520	ETKKSVVS#PEKRKLI	-1.00	0.65	0.69
<b>YDR096W</b>	<b>GIS1</b>	<b>696</b>	<b>ISREASKS#PISSFVN</b>	<b>-2.86</b>	<b>0.60</b>	<b>0.99</b>
YDR096W	GIS1	425	TTISRRISS#PLLSRMM	-1.43	0.73	0.99
<b>YLR258W</b>	<b>GSY2</b>	<b>655</b>	<b>RPLSVPGS#PRDLRSN</b>	<b>-1.65</b>	<b>2.96</b>	<b>0.43</b>
<b>YMR192W</b>	<b>GYL1</b>	<b>17</b>	<b>ERIEVPRT#PHQTQPE</b>	<b>-2.35</b>	<b>0.76</b>	<b>0.57</b>
YOR070C	GYP1	546	TPTKDFQS#PTTALSN	-3.64	0.84	0.78
YOR070C	GYP1	539	PRVASFVT#PTKDFQS	-3.64	0.84	0.78
YOR070C	GYP1	555	TTALSNMT#PNNAVED	-2.71	0.60	0.78
YDL234C	GYP7	265	DSWL TNNS#PIQKSQLI	-1.18	0.56	0.43
YJL165C	HAL5	64	IITSNVSS#PSISP V H	-1.58	0.80	0.46
YOR358W	HAP5	8	MTDRNFS#PQQGQGP	-1.03	0.72	0.43
<b>YDL223C</b>	<b>HBT1</b>	<b>671</b>	<b>KQDEDPLS#PRQTTNR</b>	<b>-1.35</b>	<b>0.56</b>	<b>0.43</b>
YDR458C	HEH2	123	MQI QEEKS#PKKKRK K	-1.53	1.97	1.70
<b>YIL112W</b>	<b>HOS4</b>	<b>690</b>	<b>KKREKTQS#PILASRR</b>	<b>-3.73</b>	<b>0.65</b>	<b>1.48</b>
<b>YIL112W</b>	<b>HOS4</b>	<b>290</b>	<b>NLSNMNSS#PAQNPKR</b>	<b>-2.89</b>	<b>0.79</b>	<b>1.48</b>
YOL123W	HRP1	462	TSNTD SGS#PPLNLPN	-1.02	0.91	0.43
YKL101W	HSL1	1220	ILSKLRLS#PENPSNT	-2.90	1.08	0.54
YHR094C	HXT1	31	GRSKAMNT#PEGKNES	-2.04	0.67	0.43
<b>YJL146W</b>	<b>IDS2</b>	<b>130</b>	<b>PEPSERAS#PIRQPSV</b>	<b>-1.10</b>	<b>0.65</b>	<b>0.43</b>
YHR132W-A	IGO2	128	SSGPPPRS#PNK	-2.83	1.27	0.43
YNL106C	INP52	1016	EISIVS VS#PRKGES N	-4.31	0.81	0.43
YNL106C	INP52	1005	EPSSKLLS#PTKEISI	-4.31	0.59	0.43
<b>YOR109W</b>	<b>INP53</b>	<b>986</b>	<b>PSTSKEKS#PTPQTST</b>	<b>-4.34</b>	<b>0.51</b>	<b>0.43</b>
YOR109W	INP53	988	TSKEKSPT#PQTSTAS	-2.25	1.46	0.43
<b>YPL209C</b>	<b>IPL1</b>	<b>76</b>	<b>MESSKIPS#PIRKATS</b>	<b>-2.10</b>	<b>1.23</b>	<b>0.68</b>
YPL242C	IQG1	49	NSSLNIAS#PSHLKTK	-5.16	1.10	0.88
YPL242C	IQG1	365	NKSLSYYS#PTISKYL	-3.41	1.13	0.88
YPL242C	IQG1	354	PTPSLEY S#PIKNKSL	-2.71	0.82	0.88

ORF	SGDB name	Site position	Context	log2 (H/L)	age precise position	age enrichment
YPL242C	IQG1	315	NCSDFSNT#PSPYNEA	-1.80	0.63	0.88
YPL242C	IQG1	404	KYSPSHYS#PMRRERM	-1.70	1.05	0.88
YPL242C	IQG1	268	NINTAPAS#PEEPKEK	-1.26	0.80	0.88
YPL242C	IQG1	317	SDFSNTPS#PYNEAPK	-1.14	0.67	0.88
YBR245C	ISW1	694	TSTGSAGT#PEPGSGE	<b>-2.32</b>	<b>1.11</b>	<b>0.43</b>
YOR304W	ISW2	1079	TSATREDT#PLSQNES	<b>-3.00</b>	<b>0.74</b>	<b>0.43</b>
YPR141C	KAR3	21	TQHLSTPS#PKNDILA	<b>-2.64</b>	<b>1.01</b>	<b>0.43</b>
YPL269W	KAR9	632	TPLSQLLS#PREGRLD	-1.11	0.93	0.92
YPL269W	KAR9	496	NPFFDPES#PNKGKLI	-1.11	0.75	0.92
YHR158C	KEL1	613	ANQIKNN#PILETLIP	<b>-3.02</b>	<b>2.21</b>	<b>1.64</b>
YHR158C	KEL1	503	APLASAPS#PAPKDFS	-2.93	0.89	1.64
YHR158C	KEL1	67	SNVNKTSS#PPMFARK	<b>-1.60</b>	<b>1.18</b>	<b>1.64</b>
YHR158C	KEL1	689	GVAQMASS#PSKDQFK	-1.16	0.87	1.64
YHR102W	KIC1	735	PLFGVGTS#PNRKPG	<b>-2.07</b>	<b>0.74</b>	<b>0.79</b>
YLR096W	KIN2	24	TSKGGSLS#PTPEAFN	<b>-3.37</b>	<b>1.01</b>	<b>1.31</b>
YLR096W	KIN2	609	IPEQAHTS#PTSRKSS	<b>-1.59</b>	<b>1.02</b>	<b>1.31</b>
YLR096W	KIN2	643	EYQQRSAS#PVVGEHQ	-1.09	0.86	1.31
YOR233W	KIN4	460	GLVTIPGS#PTTARTR	-2.37	0.77	1.32
YKL168C	KKQ8	37	PPRSRDSS#PINVTRI	-2.07	0.65	0.50
YJR070C	LIA1	281	EALGAIAS#PEVVVDVL	-1.28	0.75	0.43
YGL090W	LIF1	261	KPISELNS#PGKRMKR	-1.98	0.84	0.43
YDR439W	LRS4	146	KPTIHLLS#PIVNRDK	<b>-3.40</b>	<b>0.98</b>	<b>0.43</b>
YDR439W	LRS4	230	RLSALQKS#PELRKER	-2.94	0.51	0.43
YAL024C	LTE1	212	YARQSFAS#PDFRNQS	<b>-4.00</b>	<b>0.91</b>	<b>2.06</b>
YAL024C	LTE1	614	SEAITNMT#PRRKNHIS	<b>-2.33</b>	<b>0.81</b>	<b>2.06</b>
YDL182W	LYS20	396	NFHAEVST#PQVLSAK	-1.25	1.22	0.43
YDL131W	LYS21	410	DFHAELST#PLLKPVN	-1.00	1.25	0.43
YJL013C	MAD3	478	AVKPRQLT#PILEMRE	-2.92	0.75	0.55
YKL093W	MBR1	69	FNFQPDSS#PCNAKCQ	-2.59	0.65	0.43
YEL032W	MCM3	781	QPASNNSGS#PIKSTPR	<b>-1.90</b>	<b>0.75</b>	<b>0.43</b>
YGL197W	MDS3	1387	KSSAFTPQS#PIRAYGS	-2.90	0.84	1.03
YGL197W	MDS3	693	EDDEDPV#PKPVSKS	<b>-1.08</b>	<b>0.65</b>	<b>1.03</b>
YOR174W	MED4	237	QMAKKEGT#PKTDSFI	-1.09	0.63	0.43
YIL046W	MET30	67	KMTMATRS#PSSSPDL	-1.27	0.68	0.43
YGL035C	MIG1	264	QQQQNQLS#PRYSNTV	-2.20	0.88	2.24
YMR036C	MIH1	27	FQKISLKS#PFGKKKN	<b>-4.30</b>	<b>0.83</b>	<b>2.16</b>
YNL074C	MLF3	297	PATSPYVS#PQQSARQ	-2.97	1.18	1.07
YNL074C	MLF3	79	KNSNNVSS#PLDNVIP	<b>-2.18</b>	<b>0.65</b>	<b>1.07</b>
YNL074C	MLF3	56	FYNLQTIS#PIPISGS	-1.94	0.65	1.07
YNL074C	MLF3	265	CPFILKRS#PPQAYSS	-1.77	0.56	1.07
YNL074C	MLF3	183	SSESSPAS#PDLKLSR	<b>-1.68</b>	<b>0.65</b>	<b>1.07</b>
YNL074C	MLF3	180	TLPSSESS#PASPDLK	-1.60	0.65	1.07
YLL061W	MMP1	21	FSTSVLST#PSNEGNN	-3.83	0.63	0.43
YLR190W	MMR1	37	SFQNLLNS#PTKLKLD	<b>-1.11</b>	<b>0.83</b>	<b>0.51</b>
YIL106W	MOB1	80	ESDHGRMS#PVLTPK	<b>-4.65</b>	<b>0.65</b>	<b>0.44</b>
YIL106W	MOB1	36	ANNAGSVS#PTKATPH	<b>-1.20</b>	<b>1.07</b>	<b>0.44</b>
YFL034C-B	MOB2	76	SQQLTSTT#PQSQQQE	-1.03	1.02	0.74
YPL082C	MOT1	791	SFVSEIFS#PVMNKQL	-2.30	0.65	0.43
YLR219W	MSC3	46	ASAASAAS#PDRTNYS	<b>-1.13</b>	<b>0.65</b>	<b>0.63</b>
YDR097C	MSH6	228	YNTSHSSS#PFTRNIS	<b>-1.84</b>	<b>1.18</b>	<b>0.43</b>
YLR116W	MSL5	378	SRYAPSPS#PPASHIS	<b>-1.21</b>	<b>1.06</b>	<b>0.71</b>
YLR116W	MSL5	376	ASSRYAPS#PSPPASH	-1.21	0.74	0.71
YKL062W	MSN4	178	FNENIELS#PHQHATS	-1.58	0.79	1.42
YKL062W	MSN4	161	EQLEKVFS#PMNPIND	-1.58	0.65	1.42
YAR033W	MST28	179	TATSIGNS#PVAKPE	-1.19	0.51	0.43
YPL070W	MUK1	245	IVGTSVSS#PNKMKTF	<b>-2.42</b>	<b>0.99</b>	<b>0.43</b>
YPL070W	MUK1	67	ERLENNKNS#PILTKQE	-1.10	0.73	0.43

ORF	SGDB name	Site position	Context	log2 (H/L)	age precise position	age enrichment
YLR457C	NBP1	253	LKIDLSPS#PIRRTNS	-1.04	1.12	0.56
YLR457C	NBP1	251	KPLKIDLS#PSPIRRT	-1.04	0.94	0.56
<b>YBL024W</b>	<b>NCL1</b>	<b>426</b>	<b>TEKLSSSET#PALESEG</b>	<b>-1.76</b>	<b>0.75</b>	<b>0.43</b>
YJL076W	NET1	676	RNILPQRT#PRSAAKR	-4.43	0.84	1.05
YJL076W	NET1	1056	TQLMDMSS#PPSVVSK	-3.50	1.12	1.05
YJL076W	NET1	1042	VNKKINAT#PDKIPVT	-3.50	1.02	1.05
<b>YJL076W</b>	<b>NET1</b>	<b>1032</b>	<b>SSKIEAPS#PSVNKKI</b>	<b>-3.46</b>	<b>0.56</b>	<b>1.05</b>
YJL076W	NET1	252	PPPTQPQS#PPIRISS	-2.69	1.10	1.05
YJL076W	NET1	830	SFPVVGGG#PSVATKG	-2.49	0.64	1.05
YJL076W	NET1	447	SIADNNNGS#PVKNNSPL	-2.23	1.18	1.05
YJL076W	NET1	452	NGSPVKNS#PLGDAMP	-2.23	0.91	1.05
YJL076W	NET1	166	RSKLNNGS#PQSVQPQ	-2.13	0.65	1.05
YJL076W	NET1	297	QQRLLSGT#PIMSTM	-1.81	1.18	1.05
YOR056C	NOB1	367	GNRYSVAS#PLSKNSQ	-3.14	1.69	0.58
<b>YPR072W</b>	<b>NOT5</b>	<b>306</b>	<b>FDNSTLGT#PTTHVSM</b>	<b>-1.33</b>	<b>0.97</b>	<b>0.55</b>
YML059C	NTE1	645	RNAQLSTS#PLSLDNT	-1.12	0.66	0.44
<b>YDR001C</b>	<b>NTH1</b>	<b>66</b>	<b>MSVFDNVS#PFKKTGF</b>	<b>-5.54</b>	<b>0.75</b>	<b>0.43</b>
YOR098C	NUP1	767	HNKEKSNS#PTSFFDG	-1.13	0.89	1.29
YIL115C	NUP159	854	HVKAKSES#PFSAFAT	-1.72	1.83	2.37
YIL115C	NUP159	735	FKFGTQAS#PFSSQLG	-1.09	1.13	2.37
<b>YAR002W</b>	<b>NUP60</b>	<b>460</b>	<b>VQPDLSVT#PKSSSSK</b>	<b>-4.10</b>	<b>0.79</b>	<b>1.02</b>
<b>YAR002W</b>	<b>NUP60</b>	<b>222</b>	<b>FNYSSLPS#PYKTTVY</b>	<b>-2.35</b>	<b>1.65</b>	<b>1.02</b>
<b>YAR002W</b>	<b>NUP60</b>	<b>382</b>	<b>NVVVAETS#PEKKDGG</b>	<b>-1.47</b>	<b>1.22</b>	<b>1.02</b>
<b>YAR002W</b>	<b>NUP60</b>	<b>312</b>	<b>IRKHKRVS#PNAAPRQ</b>	<b>-1.17</b>	<b>0.60</b>	<b>1.02</b>
YHR195W	NVJ1	298	SLLHIQVS#PTKSSNL	-1.06	0.65	0.43
YHL029C	OCA5	8	MHDKKS#PMANSHY	-1.60	0.83	0.58
YBR060C	ORC2	217	LTLSRNFT#PTPVPKN	-1.30	0.87	1.08
YPR162C	ORC4	9	TISEARLS#PQVNLLP	-1.51	0.56	0.55
<b>YHR118C</b>	<b>ORC6</b>	<b>116</b>	<b>KQFAWTPS#PKKKNKRS</b>	<b>-1.12</b>	<b>1.58</b>	<b>1.30</b>
<b>YHR118C</b>	<b>ORC6</b>	<b>114</b>	<b>PMKQFAWT#PSPKKNK</b>	<b>-1.12</b>	<b>1.18</b>	<b>1.30</b>
YGR178C	PBP1	193	ERKLEKWT#PEEGAEH	-4.18	1.35	2.14
<b>YGR178C</b>	<b>PBP1</b>	<b>436</b>	<b>TPSAKTVS#PTTQISA</b>	<b>-1.95</b>	<b>0.92</b>	<b>2.14</b>
YER149C	PEA2	345	PVTWDPSS#PSSVGSP	-1.42	1.27	0.60
YML123C	PHO84	579	NNDIESSS#PSQLQHE	-1.53	0.65	0.43
YLR273C	PIG1	645	FRDYFYKS#PSP	-2.40	0.63	0.99
<b>YBL051C</b>	<b>PIN4</b>	<b>541</b>	<b>LLRNSQIS#PPNSQIP</b>	<b>-1.25</b>	<b>1.31</b>	<b>0.89</b>
<b>YBL051C</b>	<b>PIN4</b>	<b>466</b>	<b>SMQPTLTS#PKMNIHH</b>	<b>-1.01</b>	<b>0.79</b>	<b>0.89</b>
YIL122W	POG1	168	INASELAS#PRGHRRY	-2.48	0.93	0.43
YNL102W	POL1	215	KYLEIESS#PLKLQSR	-2.32	0.83	0.43
YNL102W	POL1	313	PFVTAPGT#PIGIKGL	-2.02	2.07	0.43
YNL102W	POL1	305	SRSNPSTS#PFVTAPG	-2.02	0.83	0.43
<b>YNL102W</b>	<b>POL1</b>	<b>170</b>	<b>LRENLNSS#PTSEFKS</b>	<b>-1.28</b>	<b>0.77</b>	<b>0.43</b>
YBL035C	POL12	111	FGLSIPKT#PTLKKRK	-3.50	2.60	0.65
YLR018C	POM34	221	YLFKGLET#PLKARQR	-1.68	1.18	0.85
<b>YLR018C</b>	<b>POM34</b>	<b>273</b>	<b>NDNNNSPHT#PVTRKGY</b>	<b>-1.13</b>	<b>0.65</b>	<b>0.85</b>
YIL114C	POR2	103	GDVNAFLT#PQSIKNA	-3.59	0.88	0.43
<b>YML016C</b>	<b>PPZ1</b>	<b>265</b>	<b>AYSTPLNS#PGLSKLT</b>	<b>-1.83</b>	<b>1.21</b>	<b>0.65</b>
YML016C	PPZ1	261	DGNTAYST#PLNSPGL	-1.59	1.39	0.65
YML016C	PPZ1	142	MIQMEPKS#PILKTNN	-1.54	2.41	0.65
YDR436W	PPZ2	299	NVNGRGT#PIPNLNI	-2.54	1.18	0.74
YDR436W	PPZ2	310	NLNIDKPS#PSASSAS	-2.54	0.59	0.74
YMR137C	PSO2	193	SFISNPSS#PAKTKRD	-2.99	0.64	0.43
YML017W	PSP2	340	TPLSKLDS#PALELQS	-1.19	0.75	0.46
<b>YBL046W</b>	<b>PSY4</b>	<b>434</b>	<b>TYRENISS#PLGKKSR</b>	<b>-2.48</b>	<b>1.02</b>	<b>0.43</b>
YBL046W	PSY4	347	FTNMDLTT#PKKYKHT	-1.83	1.02	0.43
YJR059W	PTK2	784	NSLRLSLGS#PSVSSSK	-2.44	0.65	2.12
YJR059W	PTK2	69	GSGGGNNS#PSSSAGA	-1.92	0.96	2.12

ORF	SGDB name	Site position	Context	log2 (H/L)	age precise position	age enrichment
YJR059W	PTK2	727	LKSMLNST#PTTPTHN	-1.25	0.86	2.12
YJR059W	PTK2	730	MNLNSTPTT#PTHNGPT	-1.25	0.73	2.12
YJR059W	PTK2	737	TPTHNGPT#PLPAKAG	-1.08	0.65	2.12
YER075C	PTP3	272	TATTPLSS#PQMNLKL	-2.45	0.65	1.14
YGR253C	PUP2	56	GVEKRATS#PLESDS	-3.33	1.35	0.43
YDR217C	RAD9	26	AIKEALHS#PLADGDM	-1.43	0.63	1.44
YDR217C	RAD9	937	KSMTNVLS#PKKHTDD	-1.21	0.63	1.44
YDR217C	RAD9	56	STNIIEGS#PKANPNP	-1.15	1.07	1.44
YJR033C	RAV1	1211	PVQKLLKS#PTKDRAY	-1.08	0.63	0.43
YLR248W	RCK2	46	DVSQITSS#PKKSFQD	-1.26	0.51	0.43
YDR195W	REF2	245	DDKNSSPS#PTASTSS	-1.67	0.61	0.43
YDR028C	REG1	898	RIVNNTPS#PAEVGAS	-1.47	0.74	1.73
YDR028C	REG1	896	SFRIVNNT#PSPAEVG	-1.47	0.63	1.73
YDR028C	REG1	421	NLDQNLNS#PDNNRFP	-1.10	0.60	1.73
YOR217W	RFC1	48	DQUESTNKT#PKKMPVS	-2.12	0.56	0.43
YOR127W	RGA1	278	SRNLLNKT#PLRNSSG	-4.58	1.73	1.92
YOR127W	RGA1	331	LLTSVLHS#PVSVNMK	-3.28	1.27	1.92
YOR127W	RGA1	291	SGQYLAKS#PSSYRQG	-2.53	1.69	1.92
YDR379W	RGA2	772	GKVLPLSPS#PKRLDYT	-2.84	0.77	1.92
YDR379W	RGA2	763	RVHDELPS#PGKVPLS	-2.84	0.65	1.92
YDR379W	RGA2	770	SPGVPLS#PSPKRLD	-2.84	0.65	1.92
YDR379W	RGA2	380	SKSMNHVS#PITRTDT	-1.48	0.60	1.92
YDR379W	RGA2	733	DLESQQRS#PNSSSGG	-1.34	0.75	1.92
YDR137W	RGP1	370	SSIIDIDS#PLEDNEF	-1.31	0.56	0.83
YKL038W	RGT1	229	SYNTVQQS#PITNKHT	-2.04	1.16	0.96
YKL038W	RGT1	469	EASSPGST#PQRSTKK	-1.85	1.05	0.96
YBR275C	RIF1	45	KTNLPPPS#PQAHMHI	-1.75	0.63	0.91
YFL033C	RIM15	1565	PTMTKFKS#PLSPANT	-1.55	1.30	3.06
YPR018W	RLF2	94	KLLCYKNS#PIQSTKY	-2.47	0.83	0.54
YPR018W	RLF2	515	QTASQSQS#PEKKQKA	-1.54	1.52	0.54
YLR371W	ROM2	171	DHPLPPMS#PRNEVYQ	-1.97	0.79	0.43
YLR371W	ROM2	216	STGSASTT#PTQARKS	-1.10	0.92	0.43
YER169W	RPH1	575	SLIKRVKS#PNIVTLN	-3.39	1.18	1.15
YER169W	RPH1	561	ISHSAPHS#PVNPnis	-1.38	0.77	1.15
YER169W	RPH1	430	SKSSGVSS#PLLSRMK	-1.08	1.18	1.15
YDR418W	RPL12B	38	KIGPLGLS#PKKVGED	-2.25	2.73	0.43
YIL153W	RRD1	341	IEQANAGS#PGREQTS	-2.00	0.60	0.52
YLR357W	RSC2	682	IPLSRVGS#PGAGGPL	-2.69	1.09	0.94
YLR357W	RSC2	243	LRDNRSTT#PSHSGTP	-1.25	0.73	0.94
YOR014W	RTS1	242	HSFERLPT#PTKLNPD	-3.54	1.45	1.12
YDR159W	SAC3	866	SDKNLIFS#PVNDEFN	-2.76	0.74	0.87
YDR159W	SAC3	600	VKPQINTS#PKRVATR	-1.27	0.66	0.87
YDR389W	SAC7	46	ENITVPRS#PTSLSRN	-1.92	0.65	2.11
YDR389W	SAC7	16	GSKIENVS#PSKGHVP	-1.49	0.80	2.11
YER129W	SAK1	966	KLSELSNS#PKQGSNN	-1.63	0.56	1.41
YER129W	SAK1	36	SSSVSLRS#PTKSSAT	-1.47	0.65	1.41
YER120W	SCS2	204	EKQTNST#PAPQNQI	-1.76	0.56	0.43
YGL056C	SDS23	405	SSSPSPST#PPVTTL	-1.32	0.60	0.92
YBR214W	SDS24	458	TAMEDPPS#PRSSAIA	-1.30	0.86	0.86
YLR166C	SEC10	485	NVDAFMHS#PRGNTHS	-1.44	0.60	0.43
YPL085W	SEC16	607	VSVPNIVS#PKPPVVK	-2.34	0.76	2.62
YPL085W	SEC16	1515	IGDSLQGS#PQRHINT	-1.43	0.65	2.62
YDL195W	SEC31	836	PSQPSMAS#PFVNKTN	-1.23	0.91	1.47
YDL195W	SEC31	980	PSSVSMVS#PPPLHKN	-1.07	1.23	1.47
YDR170C	SEC7	1240	DVWGKKAT#PTELAQE	-1.37	1.42	0.43
YOR057W	SGT1	171	NSSHSPIS#PLKIETA	-1.37	0.51	0.43
YBL058W	SHP1	315	GQQQLRLGS#PIPGESS	-1.29	2.61	0.43

ORF	SGDB name	Site position	Context	log2 (H/L)	age precise position	age enrichment
YBL058W	SHP1	322	SPIPGESS#PAEVPKN	-1.05	0.65	0.43
YDL225W	SHS1	447	SSPKFLNS#PDLPERT	-2.11	0.79	0.43
YOL004W	SIN3	304	DDPIRVTT#PMGTTTV	-1.62	2.72	0.58
YOL004W	SIN3	316	TTVNNNIS#PSGRGTT	-1.62	0.56	0.58
YDR422C	SIP1	200	SSATASPS#PTRSSSV	-1.06	0.75	0.43
YDR422C	SIP1	198	LESSATAS#PSPTRSS	-1.06	0.65	0.43
YDL042C	SIR2	23	NKVSNTVS#PTQDKDA	-1.13	0.56	0.43
YLR442C	SIR3	454	HSMNENPT#PEKGNAK	-1.13	0.88	0.64
YDR227W	SIR4	389	KRMEILKS#PHLSKSP	-2.96	0.56	0.53
YDR227W	SIR4	342	TSKKIVPS#PKKVAID	-2.04	0.51	0.53
YKR072C	SIS2	47	GKDSIINS#PVSGRQS	-1.70	0.63	1.15
YKR072C	SIS2	56	VSGRQSI#PTLSNAT	-1.33	0.65	1.15
YDR409W	SIZ1	139	SPSVIRQS#PTQRRTK	-2.41	0.75	1.67
YDR409W	SIZ1	132	PPTVQQQS#PSVIRQS	-2.41	0.66	1.67
YHR149C	SKG6	126	LPTMKDYS#PGINHLY	-1.61	0.51	0.43
YHR149C	SKG6	232	PDNFSNCT#PIRASSR	-1.61	0.60	0.43
YNL167C	SKO1	113	IISPPILT#PGGSKRL	-1.81	1.65	1.31
YNL167C	SKO1	108	QQRPTIIS#PPILTPG	-1.81	1.35	1.31
YNL167C	SKO1	94	HNDVKKDS#PSFLPGQ	-1.43	0.91	1.31
YBL007C	SLA1	437	IKKNFTKS#PSRSRSR	-2.93	0.77	0.74
YNL243W	SLA2	294	PARTPART#PTPTPPV	-1.62	2.12	0.43
YNL243W	SLA2	308	VVAEPAIS#PRPVSQR	-1.62	0.70	0.43
YNL243W	SLA2	298	PARTPTPT#PPVVAEP	-1.13	0.60	0.43
YNL243W	SLA2	296	RTPARTPT#PTPPPVA	-1.09	1.02	0.43
YGL113W	SLD3	467	IINSPVSS#PALRRVD	-4.42	1.04	0.80
YDR515W	SLF1	42	TSPWKSSS#PDSNTVI	-1.10	0.63	0.43
YBR156C	SLI15	268	KVRTVKES#PIAFKKK	-3.00	0.81	1.22
YBR156C	SLI15	144	SIHDTNKS#PVEPLNS	-1.04	0.65	1.22
YNL047C	SLM2	649	FYIENVDS#PRKSQL	-2.33	0.79	0.51
YLR086W	SMC4	128	RLELLQLS#PVKNSRV	-2.92	1.53	0.43
YLR086W	SMC4	113	YSQSPPRS#PGRSPTR	-1.98	2.01	0.43
YLR086W	SMC4	117	PPRSPGRS#PTRRLEL	-1.98	1.40	0.43
YDR006C	SOK1	193	NINNPSPS#PPPSSKQ	-1.24	0.65	0.43
YDR006C	SOK1	191	YTNINNPS#PSPPPSS	-1.24	0.64	0.43
YLL021W	SPA2	1087	SPELAKNS#PLAPIKK	-5.19	0.60	1.29
YLL021W	SPA2	585	NDVEEEES#PVKPLKI	-3.34	1.18	1.29
YLL021W	SPA2	646	EDNDKYVS#PIKAVTS	-2.55	0.72	1.29
YLL021W	SPA2	961	TAQESIKS#PEAARKL	-2.54	0.51	1.29
YLL021W	SPA2	274	KGPEQLKS#PEVQRAE	-2.09	0.65	1.29
YLL021W	SPA2	599	ITQKAINS#PIIRPSS	-2.04	0.84	1.29
YLL021W	SPA2	254	NYWDVNDS#PIIKVDK	-1.68	0.65	1.29
YLL021W	SPA2	937	EADSRVES#PGMKEQI	-1.58	0.65	1.29
YLL021W	SPA2	979	GEVDKIES#PRMVRES	-1.58	0.76	1.29
YLL021W	SPA2	1080	EPNSQIVS#PELAKNS	-1.57	0.91	1.29
YLL021W	SPA2	883	EPLGNVES#PDMDTQKV	-1.44	0.60	1.29
YLL021W	SPA2	910	EDDSRVES#PGMTGQI	-1.33	0.56	1.29
YGL093W	SPC105	356	DYAASVTT#PVKEAKD	-1.10	0.79	1.43
YPL124W	SPC29	59	RAQERMSS#PLHRLSP	-1.54	0.59	0.43
YKL042W	SPC42	357	NMSETFAT#PTPNNR	-1.23	1.18	0.90
YHR152W	SPO12	118	QLQQRFAS#PTDRLVS	-5.07	0.93	0.43
YHR152W	SPO12	125	SPTDRLVS#PCSLKLN	-5.07	0.93	0.43
YER161C	SPT2	173	KRPQKKAS#PGATLRG	-1.18	0.77	0.43
YML034W	SRC1	241	LGKLSVKT#PIKNTNR	-3.53	1.27	1.61
YML034W	SRC1	80	KMDRPSSS#PSIASPR	-3.03	0.51	1.61
YML034W	SRC1	85	SSSPSIAS#PRRSRRA	-2.60	0.51	1.61
YML034W	SRC1	291	ANGTGHST#PLSKLKV	-2.19	0.67	1.61
YKR091W	SRL3	212	RVDNVNVS#PLRWSSH	-2.87	0.80	0.83

ORF	SGDB name	Site position	Context	log2 (H/L)	age precise position	age enrichment
YCL037C	SRO9	40	PAPLPTSS#PWKLAPT	-2.84	1.10	0.52
YDR293C	SSD1	286	QQPQQQLS#PFRHRGS	-2.67	1.17	0.43
YDR293C	SSD1	267	KTRNNEYS#PGINSNW	-2.52	0.75	0.43
YDR293C	SSD1	231	RRATSNLS#PPSFKFP	-1.30	1.12	0.43
<b>YDR293C</b>	<b>SSD1</b>	<b>492</b>	<b>NDSDSLSS#PTKSGVR</b>	<b>-1.03</b>	<b>0.84</b>	<b>0.43</b>
<b>YLR006C</b>	<b>SSK1</b>	<b>195</b>	<b>LLRFASVS#PYPKFHS</b>	<b>-2.85</b>	<b>0.63</b>	<b>2.57</b>
YLR006C	SSK1	673	TDSVLVKS#PKQPIAP	-1.43	0.83	2.57
<b>YNR031C</b>	<b>SSK2</b>	<b>54</b>	<b>TQARVASS#PISPGLH</b>	<b>-2.48</b>	<b>0.91</b>	<b>0.51</b>
<b>YNR031C</b>	<b>SSK2</b>	<b>57</b>	<b>RVASSPIS#PGLHSTQ</b>	<b>-2.48</b>	<b>0.79</b>	<b>0.51</b>
YDR443C	SSN2	748	NDIPQTES#PLKTVDS	-4.10	1.01	1.07
YNL309W	STB1	72	KTLLAEIS#PAKKPLH	-5.02	1.13	1.13
YNL309W	STB1	89	TNKMTVIS#PVKFVEK	-3.35	0.79	1.13
YNL309W	STB1	99	KFVEKPNT#PPSSRQR	-2.71	1.03	1.13
YFL026W	STE2	382	NQFYQLPT#PTSSKNT	-1.15	0.92	0.43
YHL007C	STE20	203	STDIRRAT#PVSTPVI	-2.47	0.60	1.11
YHL007C	STE20	562	TPQQVAQS#PKAPAQE	-2.28	0.90	1.11
<b>YHL007C</b>	<b>STE20</b>	<b>502</b>	<b>MNSAANVS#PLKQTHA</b>	<b>-1.85</b>	<b>0.65</b>	<b>1.11</b>
YHL007C	STE20	512	KQTHAPTT#PNRTSPN	-1.53	0.65	1.11
YHL007C	STE20	517	PTTPNRTS#PNRSSIS	-1.11	0.60	1.11
YDR103W	STE5	329	SNYTFLHS#PLGHRRI	-2.83	0.65	0.96
<b>YGR008C</b>	<b>STF2</b>	<b>28</b>	<b>HTGNYGES#PNHIKKQ</b>	<b>-1.50</b>	<b>1.04</b>	<b>0.43</b>
YDL048C	STP4	191	TTGFKTIT#PSPPTQH	-1.40	0.73	1.17
YDL048C	STP4	193	GFKTITPS#PPTQHQHQS	-1.40	0.73	1.17
<b>YDR310C</b>	<b>SUM1</b>	<b>738</b>	<b>QTENTTSIS#PKKRRTE</b>	<b>-1.71</b>	<b>0.51</b>	<b>0.53</b>
YDR310C	SUM1	379	KFHQIPSS#PSNPVVSQ	-1.19	0.65	0.53
<b>YJL187C</b>	<b>SWE1</b>	<b>373</b>	<b>DTDEEIST#PTRRKSI</b>	<b>-2.17</b>	<b>1.04</b>	<b>2.89</b>
YJL187C	SWE1	111	DSRIKRWS#PFHENES	-1.58	0.93	2.89
YER111C	SWI4	806	PSKILENS#PILYRRR	-3.48	0.77	1.12
YER111C	SWI4	20	NTNHQNIT#PISKSVL	-3.22	0.65	1.12
<b>YDR146C</b>	<b>SWI5</b>	<b>522</b>	<b>INTYTTNS#PSKITRK</b>	<b>-4.00</b>	<b>1.38</b>	<b>2.61</b>
<b>YDR146C</b>	<b>SWI5</b>	<b>492</b>	<b>FVISETPS#PVLKSQS</b>	<b>-2.48</b>	<b>1.08</b>	<b>2.61</b>
YDR146C	SWI5	300	GFNDSLIS#PKKIRSN	-2.41	0.80	2.61
YDR146C	SWI5	261	SNTSFTGS#PSRRNNR	-2.14	1.50	2.61
YDR146C	SWI5	250	NSLSPMIS#PPMSNTS	-2.14	0.71	2.61
YDR146C	SWI5	664	GTSSVSSS#PIKENIN	-2.08	1.15	2.61
YDR146C	SWI5	505	QSKYEGRS#PQFGTHI	-1.70	1.11	2.61
YDR146C	SWI5	702	NGTGIMVS#PMKTNQR	-1.57	0.74	2.61
YPR095C	SYT1	297	AKNKPLLS#PSSFIRT	-1.11	0.51	1.45
<b>YMR005W</b>	<b>TAF4</b>	<b>36</b>	<b>TKPAFNLS#PGKASEL</b>	<b>-1.68</b>	<b>0.95</b>	<b>0.43</b>
<b>YMR005W</b>	<b>TAF4</b>	<b>49</b>	<b>ELSHSLPS#PSQIKST</b>	<b>-1.17</b>	<b>1.35</b>	<b>0.43</b>
YML072C	TCB3	1373	YAPVQSAS#PVVKPTD	-1.81	0.67	0.43
<b>YML072C</b>	<b>TCB3</b>	<b>1350</b>	<b>NLNSTSVT#PRASLDY</b>	<b>-1.57</b>	<b>1.04</b>	<b>0.43</b>
YPL180W	TCO89	546	KNSAAPAS#PLSNEHI	-1.86	0.65	0.43
<b>YML064C</b>	<b>TEM1</b>	<b>240</b>	<b>SPSSKAPS#PGVNT</b>	<b>-1.69</b>	<b>0.65</b>	<b>0.43</b>
YKR062W	TFA2	97	DDEDGFSS#PSKKVRP	-2.23	0.84	0.43
<b>YKL140W</b>	<b>TGL1</b>	<b>466</b>	<b>RTHSADRS#PLSVQAD</b>	<b>-1.88</b>	<b>0.65</b>	<b>0.43</b>
YKR089C	TGL4	756	SFSFSVAS#PTSRMLR	-2.83	0.76	0.43
YKR089C	TGL4	675	NSTLLTRT#PTKGDNH	-1.98	0.65	0.43
YGL049C	TIF4632	196	TPFEKEAT#PVLPANE	-4.68	1.09	1.91
YGL049C	TIF4632	301	KSGASVKT#PQHVTGS	-1.49	0.51	1.91
YNL088W	TOP2	1250	TKIKKEKT#PSVSETK	-2.52	0.93	0.43
<b>YLR183C</b>	<b>TOS4</b>	<b>98</b>	<b>KFSSKLSS#PSRHTRV</b>	<b>-2.08</b>	<b>0.77</b>	<b>2.85</b>
<b>YMR261C</b>	<b>TPS3</b>	<b>148</b>	<b>APSARVCS#PSQEASA</b>	<b>-1.53</b>	<b>0.61</b>	<b>0.52</b>
YER093C	TSC11	28	TNTTPLLT#PRHRSRDN	-2.53	0.63	0.43
<b>YML100W</b>	<b>TSL1</b>	<b>77</b>	<b>ISRSATRS#PSAFNR</b>	<b>-2.52</b>	<b>0.60</b>	<b>0.52</b>
<b>YML100W</b>	<b>TSL1</b>	<b>161</b>	<b>DSGSRIAS#PIQQQQQ</b>	<b>-1.28</b>	<b>0.60</b>	<b>0.52</b>
YML100W	TSL1	147	IPTDRIAS#PIQHEHD	-1.26	0.60	0.52

ORF	SGDB name	Site position	Context	log2 (H/L)	age precise position	age enrichment
YML100W	TSL1	135	GSVERFFS#PSSNIPT	-1.07	0.60	0.52
YOR124C	UBP2	917	EDTTGLTS#PTRVAKI	-1.18	0.63	0.43
<b>YGR184C</b>	<b>UBR1</b>	<b>300</b>	<b>PSNSPEAS#PSLAKID</b>	<b>-1.13</b>	<b>0.56</b>	<b>0.43</b>
<b>YGR184C</b>	<b>UBR1</b>	<b>296</b>	<b>AKTSPSNS#PEASPPL</b>	<b>-1.13</b>	<b>0.56</b>	<b>0.43</b>
YPL020C	ULP1	25	NPYSPLFS#PISTYRC	-1.62	0.97	1.00
YPL020C	ULP1	21	YHKKNPYS#PLFSPIS	-1.62	0.88	1.00
<b>YIL031W</b>	<b>ULP2</b>	<b>984</b>	<b>IDDVAFSS#PTRGIPR</b>	<b>-2.50</b>	<b>0.60</b>	<b>1.67</b>
<b>YIL031W</b>	<b>ULP2</b>	<b>795</b>	<b>SPETASVS#PPIRHNI</b>	<b>-1.03</b>	<b>0.65</b>	<b>1.67</b>
<b>YIL031W</b>	<b>ULP2</b>	<b>788</b>	<b>EDPVRAAS#PETAVS</b>	<b>-1.03</b>	<b>0.51</b>	<b>1.67</b>
YML029W	USA1	376	PPDTRSQS#PVSFAPT	-1.40	0.77	0.43
<b>YIL135C</b>	<b>VHS2</b>	<b>301</b>	<b>TGAALLSRS#PSNQQYL</b>	<b>-1.47</b>	<b>1.04</b>	<b>1.11</b>
YOR054C	VHS3	225	RSRSNSTS#PRPSVVV	-1.48	1.20	1.13
<b>YLR410W</b>	<b>VIP1</b>	<b>1107</b>	<b>FTPVNITS#PNLSFQK</b>	<b>-2.33</b>	<b>1.58</b>	<b>0.89</b>
YLL040C	VPS13	1379	SESERTAT#PQLSQLGS	-1.32	0.63	0.43
YLR337C	VRP1	703	ISKNPTKS#PPPPPSP	-1.24	0.51	0.98
YLR337C	VRP1	709	KSPPPPPS#PSTMDTG	-1.17	0.51	0.98
YML076C	WAR1	126	KRKPRRSRS#PTPFESP	-1.03	0.60	0.68
YOR083W	WHI5	154	RRSEVFLS#PSPRLRS	-6.54	1.18	1.11
YOR083W	WHI5	156	SEVFLSPS#PRLRSPP	-6.54	1.11	1.11
YOR083W	WHI5	88	SLQGIFMS#PVNKRRV	-2.95	0.99	1.11
YOR083W	WHI5	161	SPSPRLRS#PPTAARR	-2.75	1.18	1.11
<b>YOR083W</b>	<b>WHI5</b>	<b>62</b>	<b>FGTPSPPS#PPGITKS</b>	<b>-1.97</b>	<b>1.12</b>	<b>1.11</b>
YOR083W	WHI5	57	RLKNGFGT#PSPPSPP	-1.97	1.04	1.11
YOR083W	WHI5	59	KNGFGTPS#PPSPPGI	-1.97	0.65	1.11
YHL028W	WSC4	541	RTSTFLHS#PIQKQHE	-2.25	0.60	1.18
YDR369C	XRS2	349	RAPEVEAS#PVVSKKR	-2.34	0.65	0.43
<b>YBL005W-AYBL005W-A</b>	<b>409</b>		<b>NVSTFNNS#PGPDNDL</b>	<b>-1.03</b>	<b>0.51</b>	<b>0.53</b>
YCL019W	YCL019W	1014	TVESDTTS#PRHSSTF	-1.68	0.51	0.49
<b>YDL089W</b>	<b>YDL089W</b>	<b>441</b>	<b>NRPSKSLS#PLRKTPL</b>	<b>-3.67</b>	<b>1.09</b>	<b>1.07</b>
<b>YDL089W</b>	<b>YDL089W</b>	<b>446</b>	<b>SLSPLRKT#PLSARQK</b>	<b>-3.67</b>	<b>1.05</b>	<b>1.07</b>
<b>YDL089W</b>	<b>YDL089W</b>	<b>474</b>	<b>DINSILRS#PKKKKNY</b>	<b>-2.40</b>	<b>1.32</b>	<b>1.07</b>
YDL156W	YDL156W	99	NQLLKMGS#PDGQDKN	-1.13	0.64	0.43
YDL173W	YDL173W	148	SLHATTSS#PNNNNAPI	-2.33	0.65	0.52
<b>YDL173W</b>	<b>YDL173W</b>	<b>246</b>	<b>GGAGNIIS#PKSSRNT</b>	<b>-1.67</b>	<b>1.05</b>	<b>0.52</b>
YDR089W	YDR089W	238	NNSSLPAS#PRSIPLL	-1.29	0.95	0.43
YDR239C	YDR239C	63	APDIPPRS#PNRNAHS	-2.10	0.65	0.63
<b>YDR348C</b>	<b>YDR348C</b>	<b>121</b>	<b>SATDFRRS#PPPVSRN</b>	<b>-1.35</b>	<b>0.85</b>	<b>0.64</b>
YEL043W	YEL043W	847	RRSFHASS#PPFNSIW	-1.12	0.91	0.54
YEL043W	YEL043W	862	NSNTNQLS#PPLEEQY	-1.12	0.51	0.54
<b>YER079W</b>	<b>YER079W</b>	<b>41</b>	<b>DLDQRSMS#PSNIASG</b>	<b>-1.41</b>	<b>0.65</b>	<b>0.43</b>
YFL042C	YFL042C	149	ATIAEIGS#PLQQVEK	-2.44	0.75	0.80
YFL042C	YFL042C	103	SFKSNVPS#PVSRSTT	-1.21	0.65	0.80
YFL042C	YFL042C	110	SPVSRSTT#PTSPVPSQ	-1.01	0.65	0.80
<b>YGR125W</b>	<b>YGR125W</b>	<b>42</b>	<b>RASVAMS#PPLCRSY</b>	<b>-1.11</b>	<b>0.65</b>	<b>0.43</b>
YGR237C	YGR237C	117	PSKSYLRS#PSVERS	-3.13	0.61	0.47
<b>YHR159W</b>	<b>YHR159W</b>	<b>236</b>	<b>HLDPSLNT#PVKNRAF</b>	<b>-3.11</b>	<b>0.80</b>	<b>0.81</b>
<b>YHR159W</b>	<b>YHR159W</b>	<b>244</b>	<b>PVKNRAFS#PVYQNIP</b>	<b>-2.72</b>	<b>0.80</b>	<b>0.81</b>
<b>YHR159W</b>	<b>YHR159W</b>	<b>29</b>	<b>RNSIIMS#PVRKTGR</b>	<b>-2.38</b>	<b>0.77</b>	<b>0.81</b>
<b>YHR159W</b>	<b>YHR159W</b>	<b>286</b>	<b>TNQSRSVS#PQDIQER</b>	<b>-1.02</b>	<b>0.80</b>	<b>0.81</b>
YIL024C	YIL024C	107	QLMDIPLS#PHTRSNT	-1.99	0.65	0.43
<b>YIR007W</b>	<b>YIR007W</b>	<b>594</b>	<b>YHDTRAKT#PTPEPSP</b>	<b>-1.38</b>	<b>0.97</b>	<b>0.43</b>
YIR007W	YIR007W	596	DTRAKTPT#PEPSPAS	-1.14	0.61	0.43
YJL193W	YJL193W	247	SGFSRQES#PLPLYEK	-3.69	1.01	0.72
YKL105C	YKL105C	980	SWTFGLPS#PLKRRTS	-3.65	0.65	0.62
YKR077W	YKR077W	147	QPAATAPS#PLVSNII	-2.19	0.65	0.58
YKR077W	YKR077W	157	VSNIIKPS#PKKLASP	-2.19	0.65	0.58
YLL032C	YLL032C	762	NTSQSGAS#PQRHKMP	-1.87	0.51	0.58

ORF	SGDB name	Site position	Context	log2 (H/L)	age precise position	age enrichment
YLR049C	YLR049C	80	QGSPVAPS#PNHRSTM	-1.24	0.59	0.43
YMR086W	YMR086W	675	HSAIPLGT#PEKGKPK	-3.94	0.77	0.78
YMR086W	YMR086W	870	QKENNVVS#PGVSSPN	-1.91	0.56	0.78
YMR086W	YMR086W	658	SIRSNSPS#PPEKINN	-1.62	0.79	0.78
<b>YMR124W</b>	<b>YMR124W</b>	<b>586</b>	<b>FSSTFSDS#PSKQRII</b>	<b>-1.71</b>	<b>0.94</b>	<b>0.83</b>
YMR196W	YMR196W	1081	IDPMMDPMS#PLNKDVS	-1.25	0.60	0.43
YMR233W	YMR233W	113	RKKKKNDS#PDNSNS	-3.86	0.60	0.43
YMR291W	YMR291W	538	NEVDLLT#PRTASMS	-1.31	0.65	0.43
<b>YNL058C</b>	<b>YNL058C</b>	<b>292</b>	<b>SATSNTSS#PKKAHKR</b>	<b>-1.63</b>	<b>0.90</b>	<b>0.62</b>
<b>YNL224C</b>	<b>YNL224C</b>	<b>345</b>	<b>NNLLPSPS#PQLTEDI</b>	<b>-2.60</b>	<b>0.79</b>	<b>0.43</b>
YNL224C	YNL224C	343	ADNNNLPS#PSPQLTE	-2.60	0.65	0.43
<b>YNL321W</b>	<b>YNL321W</b>	<b>118</b>	<b>VPDLNTAT#PSSPKRM</b>	<b>-1.97</b>	<b>0.83</b>	<b>0.43</b>
<b>YNL321W</b>	<b>YNL321W</b>	<b>121</b>	<b>LNTATPSS#PKRMHSS</b>	<b>-1.97</b>	<b>0.65</b>	<b>0.43</b>
YNR047W	YNR047W	201	GRRRSRST#PIMPSQN	-2.09	1.35	1.32
YNR047W	YNR047W	198	TGTGRRRS#PSTPIMP	-2.09	1.09	1.32
YNR047W	YNR047W	175	REHSNCGS#PIMLSSS	-1.56	0.65	1.32
<b>YNR047W</b>	<b>YNR047W</b>	<b>339</b>	<b>LKDTLNGS#PSRGSSK</b>	<b>-1.48</b>	<b>1.08</b>	<b>1.32</b>
<b>YNR047W</b>	<b>YNR047W</b>	<b>137</b>	<b>MTSVANAS#PASPPLS</b>	<b>-1.38</b>	<b>0.84</b>	<b>1.32</b>
<b>YNR047W</b>	<b>YNR047W</b>	<b>140</b>	<b>VANASPAS#PPLSPTI</b>	<b>-1.00</b>	<b>1.33</b>	<b>1.32</b>
<b>YNR047W</b>	<b>YNR047W</b>	<b>144</b>	<b>SPASPPLS#PTIPETD</b>	<b>-1.00</b>	<b>1.09</b>	<b>1.32</b>
YOL070C	YOL070C	403	YEDIIEET#PKKTKLK	-1.14	0.65	0.61
YOR227W	YOR227W	61	VPTKTIAS#PQRPLSG	-1.02	0.68	0.72
YML027W	YOX1	324	NPQKKTLT#PVKTSPN	-1.42	1.35	2.07
YPL141C	YPL141C	441	LSHEQSLS#PVQNIRQ	-1.44	0.56	1.55
YPL150W	YPL150W	456	YSHSIAGS#PRKSNNF	-1.09	0.65	0.71
<b>YPR091C</b>	<b>YPR091C</b>	<b>676</b>	<b>SQPLNTLS#PKLEGKR</b>	<b>-1.13</b>	<b>0.73</b>	<b>1.35</b>
YPR115W	YPR115W	969	ARRGSDLS#PFEMESP	-3.18	0.51	0.80
YPR115W	YPR115W	975	LSPFEMES#PLFEENR	-2.70	0.65	0.80
<b>YPR174C</b>	<b>YPR174C</b>	<b>170</b>	<b>VNPLVTSS#PIHMSPL</b>	<b>-2.85</b>	<b>1.12</b>	<b>0.49</b>
<b>YPR174C</b>	<b>YPR174C</b>	<b>175</b>	<b>TSSPIHMS#PLQSRQR</b>	<b>-2.85</b>	<b>0.65</b>	<b>0.49</b>
YIL063C	YRB2	31	PIDKLDGT#PKRPREK	-1.24	0.56	0.72
<b>YHR016C</b>	<b>YSC84</b>	<b>311</b>	<b>EDYDYGRS#PNRNSSR</b>	<b>-2.60</b>	<b>0.63</b>	<b>0.43</b>
YDR326C	YSP2	572	FLNRRSFS#PSNLGNK	-1.20	1.08	0.74
YNR039C	ZRG17	58	QNRTFFAS#PRPSSLF	-2.51	1.23	0.76
YER033C	ZRG8	914	LNRRTLKS#PLRGGSK	-4.46	1.20	1.19

**Table S2. (Following pages)** Cdk1-dependent phosphorylation sites identified in multiple biological experiments. This table lists phosphorylation sites in peptides that declined in abundance by at least 50% following Cdk1 inhibition in one experiment and also declined after Cdk1 inhibition in another experiment (as indicated by bold font in Table S1; see Dataset S2 for details). Column labels and formatting as in Table S1.

ORF	SGDB name	Site position	Context	log2 (H/L)	age precise position	age enrichment
YCR088W	ABP1	165	PPVKKSFT#PSKSPAP	-3.06	1.68	0.95
YCR088W	ABP1	169	KSFTPSKS#PAPVSKK	-3.06	0.63	0.95
YCR088W	ABP1	181	SKKEPVKT#PSPAPAA	-1.74	0.61	0.95
YCR088W	ABP1	183	KEPVKTPS#PAPAAKI	-1.32	0.63	0.95
YLR131C	ACE2	486	IPGSSNNT#PIKNSLP	-3.51	1.76	2.72
YLR131C	ACE2	392	SPGGLSIS#PRINGNS	-3.28	0.78	2.72
YLR131C	ACE2	80	LDIPLVPS#PKTGDGs	-1.27	0.77	2.72
YLR131C	ACE2	253	NSNSKPGS#PVILKTP	-1.06	0.78	2.72
YJR083C	ACF4	71	QRSTTNQS#PVSDHAS	-1.38	1.00	0.69
YBR059C	AKL1	504	DPTISEQS#PRLNTQS	-2.86	0.60	1.40
YBR059C	AKL1	801	EALLIELS#PLKEDAG	-1.54	0.87	1.40
YJL084C	ALY2	213	NGPSRNLS#PINLLKR	-2.27	1.68	1.65
YJL020C	BBC1	103	KDLPEPIS#PETKKET	-1.03	0.51	1.10
YFL007W	BLM10	29	QLKRFERS#PGRPSSS	-1.95	0.76	0.43
YER114C	BOI2	519	QGGGKALS#PIPSPTR	-1.07	0.73	2.79
YER114C	BOI2	523	KALSPIPS#PTRNSVR	-1.07	0.65	2.79
YPR171W	BSP1	309	KPKPTPPS#PPAKRIP	-1.10	0.63	0.77
YCL014W	BUD3	1440	PVEELPNT#PRSINVT	-1.78	0.61	0.90
YLR319C	BUD6	327	IDDVSKAS#PLAKTPL	-1.17	0.61	0.66
YAL038W	CDC19	407	VLSTSGTT#PRLVSKY	-1.89	1.23	0.43
YLR314C	CDC3	503	ELSINSAS#PNVNHS	-2.24	0.63	0.43
YLR314C	CDC3	509	ASPVNVHS#PVPTKKK	-1.67	1.25	0.43
YPL160W	CDC60	142	EEEIKEET#PAEKDHE	-1.52	0.63	0.43
YOR042W	CUE5	364	AETTYIDT#PDTEKK	-1.68	1.44	0.43
YER088C	DOT6	491	DMLSPTHS#PKTLSK	-2.00	0.95	1.80
YBL101C	ECM21	1030	DKLLSTPS#PVNRSHN	-1.89	0.91	1.07
YMR219W	ESC1	1145	DRSNIFSS#PIRVIGA	-1.69	0.63	0.43
YNL068C	FKH2	833	ETKDNINSS#PLKNQGG	-1.51	0.60	2.34
YAL035W	FUN12	386	AKSTPAAT#PAATPTP	-1.07	0.63	0.43
YDL226C	GCS1	170	LENRRSAT#PANSSNG	-4.40	1.11	0.43
YDL226C	GCS1	161	VAQSREGT#PLENRRS	-1.32	1.89	0.43
YDR309C	GIC2	337	AFFPSRQS#PLPKRRN	-3.37	0.79	0.85
YDR096W	GIS1	696	ISREASKS#PISSFVN	-2.86	0.60	0.99
YLR258W	GSY2	655	RPLSVPGS#PRDLRSN	-1.65	2.96	0.43
YMR192W	GYL1	17	ERIEVPRT#PHQTQPE	-2.35	0.76	0.57
YJL146W	IDS2	130	PEPSERAS#PIRQPSV	-1.10	0.65	0.43
YOR109W	INP53	986	PSTSKEKS#PTPQTST	-4.34	0.51	0.43
YBR245C	ISW1	694	TSTGSAGT#PEPGSGE	-2.32	1.11	0.43
YOR304W	ISW2	1079	TSATREDT#PLSQNES	-3.00	0.74	0.43
YHR102W	KIC1	735	PLFGVGTS#PNRKPG	-2.07	0.74	0.79
YLR096W	KIN2	609	IPEQAHTS#PTSRKSS	-1.59	1.02	1.31
YEL032W	MCM3	781	QPASNNGS#PIKSTPR	-1.90	0.75	0.43
YGL197W	MDS3	693	EDDEDPV#PKVSKS	-1.08	0.65	1.03
YNL074C	MLF3	79	KNSNNVSS#PLDNVIP	-2.18	0.65	1.07
YNL074C	MLF3	183	SSESSPAS#PDLKLSR	-1.68	0.65	1.07
YIL106W	MOB1	80	ESDHGRMS#PVLTPK	-4.65	0.65	0.44
YIL106W	MOB1	36	ANNAGSVS#PTKATPH	-1.20	1.07	0.44
YDR097C	MSH6	228	YNTSHSSS#PFTRNIS	-1.84	1.18	0.43
YLR116W	MSL5	378	SRYAPSPS#PPASHIS	-1.21	1.06	0.71
YPL070W	MUK1	245	IVGTSVSS#PNKMKTF	-2.42	0.99	0.43
YBL024W	NCL1	426	TEKLSET#PALESEG	-1.76	0.75	0.43
YJL076W	NET1	1032	SSKIEAPS#PSVNKKI	-3.46	0.56	1.05
YPR072W	NOT5	306	FDNSTLGT#PTTHVSM	-1.33	0.97	0.55
YAR002W	NUP60	222	FNYSSLPS#PYKTTVY	-2.35	1.65	1.02
YAR002W	NUP60	382	NVVVAETS#PEKKDGG	-1.47	1.22	1.02
YHR118C	ORC6	116	KQFAWTPS#PKKNKRS	-1.12	1.58	1.30
YHR118C	ORC6	114	PMKQFAWT#PSPKKNK	-1.12	1.18	1.30

ORF	SGDB name	Site position	Context	log2 (H/L)	age precise position	age enrichment
YGR178C	PBP1	436	TPSAKTVS#PTTQISA	-1.95	0.92	2.14
YBL051C	PIN4	541	LLRNSQIS#PPNSQIP	-1.25	1.31	0.89
YBL051C	PIN4	466	SMQPTLTS#PKMNIHH	-1.01	0.79	0.89
YNL102W	POL1	170	LRENLNSS#PTSEFKS	-1.28	0.77	0.43
YLR018C	POM34	273	NDNNNSPHT#PVTRKGY	-1.13	0.65	0.85
YML016C	PPZ1	265	AYSTPLNS#PGLSKLT	-1.83	1.21	0.65
YBL046W	PSY4	434	TYRENISS#PLGKKSR	-2.48	1.02	0.43
YJR059W	PTK2	727	LKSMLNST#PTTPTHN	-1.25	0.86	2.12
YJR059W	PTK2	730	MLNSTPTT#PTHNGPT	-1.25	0.73	2.12
YJR059W	PTK2	737	TPTHNGPT#PLPAKAG	-1.08	0.65	2.12
YDR217C	RAD9	26	AIKEALHS#PLADGDM	-1.43	0.63	1.44
YDR217C	RAD9	56	STNIIEGS#PKANPNP	-1.15	1.07	1.44
YJR033C	RAV1	1211	PVQKLKKS#PTKDRAY	-1.08	0.63	0.43
YLR248W	RCK2	46	DVSQITSS#PKKSFQD	-1.26	0.51	0.43
YDR028C	REG1	421	NLDQNLNS#PDNNRFP	-1.10	0.60	1.73
YPR018W	RLF2	94	KLLCYKNS#PIQSTKY	-2.47	0.83	0.54
YER169W	RPH1	575	SLIKRVK5#PNIVTLN	-3.39	1.18	1.15
YER169W	RPH1	561	ISHSAPHS#PVNPNPIS	-1.38	0.77	1.15
YER169W	RPH1	430	SKSSGVSS#PLLSRMK	-1.08	1.18	1.15
YDR418W	RPL12B	38	KIGPLGLS#PKKVGED	-2.25	2.73	0.43
YLR357W	RSC2	682	IPLSRVGS#PGAGGPL	-2.69	1.09	0.94
YLR357W	RSC2	243	LRDNRSTT#PSHSGTP	-1.25	0.73	0.94
YDR159W	SAC3	600	VKPQINTS#PKRVATR	-1.27	0.66	0.87
YER129W	SAK1	966	KLSELNSNS#PKQKGSNN	-1.63	0.56	1.41
YGL056C	SDS23	405	SSSPSPST#PPVTTLP	-1.32	0.60	0.92
YBR214W	SDS24	458	TAMEDPPS#PRSSAIA	-1.30	0.86	0.86
YPL085W	SEC16	1515	IGDSLQGS#PQRHINT	-1.43	0.65	2.62
YDR170C	SEC7	1240	DVWGKKAT#PTELAQE	-1.37	1.42	0.43
YBL058W	SHP1	315	GQQQRLGS#PIPGESSION	-1.29	2.61	0.43
YBL058W	SHP1	322	SPIPGESS#PAEVPKN	-1.05	0.65	0.43
YDL225W	SHS1	447	SSPKFLNS#PDLPERT	-2.11	0.79	0.43
YOL004W	SIN3	304	DDPIRVTT#PMGTTTV	-1.62	2.72	0.58
YOL004W	SIN3	316	TTVNNNNIS#PSGRGTT	-1.62	0.56	0.58
YDL042C	SIR2	23	NKVSNTVS#PTQDKDA	-1.13	0.56	0.43
YKR072C	SIS2	56	VSGRQNSIS#PTLSNAT	-1.33	0.65	1.15
YNL243W	SLA2	294	PARTPART#PTPTPPV	-1.62	2.12	0.43
YNL243W	SLA2	308	VVAEPAIS#PRPVVSQR	-1.62	0.70	0.43
YNL243W	SLA2	298	PARTPTPT#PPVVAEP	-1.13	0.60	0.43
YNL243W	SLA2	296	RTPARTPT#PTPPPVA	-1.09	1.02	0.43
YDR515W	SLF1	42	TSPWKSSS#PDSNTVI	-1.10	0.63	0.43
YNL047C	SLM2	649	FYIENVDS#PRKSNQL	-2.33	0.79	0.51
YLR086W	SMC4	113	YSQSPPRS#PGRSPTR	-1.98	2.01	0.43
YDR006C	SOK1	193	NINNPSPS#PPPSSKQ	-1.24	0.65	0.43
YDR006C	SOK1	191	YTNINNPS#PSPPPSS	-1.24	0.64	0.43
YLL021W	SPA2	585	NDVEEEES#PVKPLKI	-3.34	1.18	1.29
YLL021W	SPA2	599	ITQKAINS#PIIRPSS	-2.04	0.84	1.29
YLL021W	SPA2	254	NYWDVNDNS#PIIKVDK	-1.68	0.65	1.29
YLL021W	SPA2	979	GEVDKIES#PRMVRES	-1.58	0.76	1.29
YLL021W	SPA2	883	EPLGNVES#PDMDTQKV	-1.44	0.60	1.29
YDR293C	SSD1	492	NDSDSLSS#PTKSGVR	-1.03	0.84	0.43
YLR006C	SSK1	195	LLRFASVS#PYPKFHS	-2.85	0.63	2.57
YNR031C	SSK2	54	TQARVASS#PISPGLH	-2.48	0.91	0.51
YNR031C	SSK2	57	RVASSPIS#PGLHSTQ	-2.48	0.79	0.51
YHL007C	STE20	502	MNSAANVS#PLKQTHA	-1.85	0.65	1.11
YGR008C	STF2	28	HTGNYGES#PNHIKKQ	-1.50	1.04	0.43
YDR310C	SUM1	738	QTENTTS#PKKRRTE	-1.71	0.51	0.53
YDR146C	SWI5	492	FVISETPS#PVLKSQLS	-2.48	1.08	2.61

ORF	SGDB name	Site position	Context	log2 (H/L)	age precise position	age enrichment
YML072C	TCB3	1350	NLNSTSVT#PRASLDY	-1.57	1.04	0.43
YML064C	TEM1	240	SPSSKAPS#PGVNT	-1.69	0.65	0.43
YKL140W	TGL1	466	RTHSADRS#PLSVQAD	-1.88	0.65	0.43
YMR261C	TPS3	148	APSARVCS#PSQEASA	-1.53	0.61	0.52
YML100W	TSL1	77	ISRSATRS#PSAFNRA	-2.52	0.60	0.52
YML100W	TSL1	161	DSGSRIAS#PIQQQQQ	-1.28	0.60	0.52
YML100W	TSL1	147	IPTDRIAS#PIQHEHD	-1.26	0.60	0.52
YGR184C	UBR1	300	PSNSPEAS#PSLAKID	-1.13	0.56	0.43
YGR184C	UBR1	296	AKTSPSNS#PEASPSL	-1.13	0.56	0.43
YIL031W	ULP2	984	IDDVAFSS#PTRGIPR	-2.50	0.60	1.67
YML029W	USA1	376	PPDTRSQS#PVSFAPT	-1.40	0.77	0.43
YIL135C	VHS2	301	TGAALSRSL#PSNQQYL	-1.47	1.04	1.11
YLR410W	VIP1	1107	FTPVNITS#PNLSFQK	-2.33	1.58	0.89
YLL040C	VPS13	1379	SESERTAT#PQLSQGS	-1.32	0.63	0.43
YLR337C	VRP1	703	ISKNPTKS#PPPPPSP	-1.24	0.51	0.98
YLR337C	VRP1	709	KSPPPPPS#PSTMGTG	-1.17	0.51	0.98
YOR083W	WHI5	62	FGTPSPPS#PPGITKS	-1.97	1.12	1.11
YBL005W-AYBL005W-A		409	NVSTFNNS#PGPDNDL	-1.03	0.51	0.53
YDL173W	YDL173W	246	GGAGNIIS#PKSSRNT	-1.67	1.05	0.52
YDR348C	YDR348C	121	SATDFRRS#PPPVSRN	-1.35	0.85	0.64
YER079W	YER079W	41	DLDQRSMS#PSNIASG	-1.41	0.65	0.43
YGR125W	YGR125W	42	RASVSAMS#PPLCRSY	-1.11	0.65	0.43
YHR159W	YHR159W	286	TNQSRSVS#PQDIQER	-1.02	0.80	0.81
YIR007W	YIR007W	594	YHDTRAKT#PTPEPSP	-1.38	0.97	0.43
YMR124W	YMR124W	586	FSSTFSDS#PSKQRII	-1.71	0.94	0.83
YNL058C	YNL058C	292	SATSNTSS#PKKAHKR	-1.63	0.90	0.62
YNL224C	YNL224C	345	NNLLPSPS#PQLTEIDI	-2.60	0.79	0.43
YNL321W	YNL321W	121	LNTATPSS#PKRMHSS	-1.97	0.65	0.43
YNR047W	YNR047W	339	LKDTLNGS#PSRGSSK	-1.48	1.08	1.32
YNR047W	YNR047W	137	MTSVANAS#PASPLS	-1.38	0.84	1.32
YNR047W	YNR047W	140	VANASPAS#PPLSPTI	-1.00	1.33	1.32
YNR047W	YNR047W	144	SPASPLS#PTIPETD	-1.00	1.09	1.32
YPR091C	YPR091C	676	SQPLNTLS#PKLEGKR	-1.13	0.73	1.35
YPR174C	YPR174C	170	VNPVLTSS#PIHMSPL	-2.85	1.12	0.49
YPR174C	YPR174C	175	TSSPIHMS#PLQSRQR	-2.85	0.65	0.49
YIL063C	YRB2	31	PIDKLDGT#PKRPREK	-1.24	0.56	0.72
YHR016C	YSC84	311	EDYDYGRS#PNRNSSR	-2.60	0.63	0.43
YDR326C	YSP2	572	FLNRRSFS#PSNLGNK	-1.20	1.08	0.74

GOID	Gene Ontology Term	Frequency	Background	P-value
7049	cell cycle	74/308 24.0%	472/7163 6.6%	3.61E-21
278	mitotic cell cycle	53/308 17.2%	287/7163 4.0%	1.36E-17
7346	regulation of mitotic cell cycle	24/308 7.8%	75/7163 1.0%	1.56E-12
51726	regulation of cell cycle	34/308 11.0%	161/7163 2.2%	2.48E-12
902	cell morphogenesis	32/308 10.4%	151/7163 2.1%	1.52E-11
910	cytokinesis	27/308 8.8%	117/7163 1.6%	2.05E-10
33043	regulation of organelle organization	26/308 8.4%	111/7163 1.5%	3.96E-10
30010	establishment of cell polarity	25/308 8.1%	106/7163 1.5%	9.55E-10
51783	regulation of nuclear division	18/308 5.8%	52/7163 0.7%	1.17E-09
19954	asexual reproduction	22/308 7.1%	84/7163 1.2%	2.29E-09
7114	cell budding	22/308 7.1%	84/7163 1.2%	2.29E-09
7096	regulation of exit from mitosis	12/308 3.9%	24/7163 0.3%	3.68E-08
30036	actin cytoskeleton organization	21/308 6.8%	101/7163 1.4%	7.73E-07
6270	DNA replication initiation	12/308 3.9%	35/7163 0.5%	7.41E-06
8361	regulation of cell size	21/308 6.8%	117/7163 1.6%	1.25E-05

**Table S3.** Gene ontology analysis of Cdk1 substrates. The set of proteins defined as Cdk1 substrates by our quantitative mass spectrometry experiments were assessed for enrichment in Gene Ontology categories (20).

		Non-Phosphopeptides		Phosphopeptides				
		all proteins	motif matches in all proteins	proteins sampled in experiment	false instances (all S/Ts)	proteins sampled in experiment	motif matches in proteins sampled in experiment	true instances
PsiPred	Helix Residue Count	1,145,218	1,020	630,388	12,587	72,048	64	35
	Sheet Residue Count	324,753	521	188,986	4,518	20,525	29	1
	Loop Residue Count	1,442,764	18,500	787,782	20,635	155,838	2,874	511
	Helix Residue Fraction	39.3%	5.1%	39.2%	33.4%	29.0%	2.2%	6.4%
	Sheet Residue Fraction	11.1%	2.6%	11.8%	12.0%	8.3%	1.0%	0.2%
	Loop Residue Fraction	49.5%	92.3%	49.0%	54.7%	62.7%	96.9%	93.4%
PONDR	Disorder Residue Count	1,143,370	12,662	604,523	16,591	145,079	2,501	535
	Disorder Residue Fraction	37.7%	60.6%	37.7%	44.0%	58.6%	84.6%	98.5%
PFam	Residues In Domain Count	1,092,024	6,007	664,421	18,620	61,465	375	32
	Residues In Domain Fraction	38.2%	30.5%	41.3%	49.3%	24.7%	12.6%	5.9%

**Table S4.** Phosphorylation sites are located in loops and disordered regions, outside of predicted protein domains. Analysis of the placement of Cdk1 phosphorylation sites in predicted secondary structure (top, PsiPred), predicted intrinsically ordered/disordered regions (middle, PONDR), and predicted domains (bottom, Pfam) (10-14). Each column refers to a particular subset of residues, as follows: “all proteins” indicates all residues in all proteins in the yeast proteome; ‘motif matches in all proteins’ indicates all serines and threonines in the yeast proteome that are followed by a proline; ‘proteins sampled in experiment’ indicates all residues in all peptides analyzed in our experiments (nonphosphopeptides on the left, phosphopeptides on the right); ‘motif matches in proteins sampled in experiment’ indicates all serines and threonines followed by a proline in all phosphopeptides, whether they were detectably phosphorylated or not; and “true instances” indicates the 547 serines and threonines that we identified as Cdk1-dependent phosphorylation sites. Values indicate the number of residues of a given type; for example, the count in the upper-leftmost cell of the table indicates the number of all residues across all proteins that fall within predicted helices, and fractions are the relative frequency of that residue type. The comparison of all proteins with all nonphosphopeptides sampled in our experiment indicates that there is no intrinsic bias in recovery or detection of different protein regions during cell lysis, protein recovery, digestion, and LC-MS/MS. Values for all proteins and true instances are plotted in Fig. 3A.

protein length	Expected	# of consensus motif instances found in protein												
		0	1	2	3	4	5	6	7	8	9	10	11	12
		p-value												
50	0.355	1.0E+00	3.0E-01	5.0E-02	5.7E-03	5.0E-04	3.5E-05	2.1E-06	1.0E-07	4.6E-09	1.8E-10	6.3E-12	2.0E-13	0.0E+00
100	0.71	1.0E+00	5.1E-01	1.6E-01	3.5E-02	6.0E-03	8.4E-04	9.7E-05	9.7E-06	8.5E-07	6.7E-08	4.7E-09	3.0E-10	1.8E-11
150	1.065	1.0E+00	6.6E-01	2.9E-01	9.3E-02	2.3E-02	4.8E-03	8.2E-04	1.2E-04	1.6E-05	1.9E-06	2.0E-07	1.9E-08	1.7E-09
200	1.42	1.0E+00	7.6E-01	4.2E-01	1.7E-01	5.6E-02	1.5E-02	3.4E-03	6.8E-04	1.2E-04	1.8E-05	2.5E-06	3.2E-07	3.8E-08
250	1.775	1.0E+00	8.3E-01	5.3E-01	2.6E-01	1.0E-01	3.5E-02	9.7E-03	2.4E-03	5.1E-04	9.9E-05	1.7E-05	2.7E-06	4.0E-07
300	2.13	1.0E+00	8.8E-01	6.3E-01	3.6E-01	1.7E-01	6.5E-02	2.2E-02	6.3E-03	1.6E-03	3.7E-04	7.8E-05	1.5E-05	2.6E-06
350	2.485	1.0E+00	9.2E-01	7.1E-01	4.5E-01	2.4E-01	1.1E-01	4.1E-02	1.4E-02	4.1E-03	1.1E-03	2.6E-04	5.8E-05	1.2E-05
400	2.84	1.0E+00	9.4E-01	7.8E-01	5.4E-01	3.2E-01	1.6E-01	6.9E-02	2.6E-02	8.8E-03	2.7E-03	7.3E-04	1.8E-04	4.3E-05
450	3.195	1.0E+00	9.6E-01	8.3E-01	6.2E-01	4.0E-01	2.2E-01	1.0E-01	4.4E-02	1.7E-02	5.7E-03	1.7E-03	4.9E-04	1.3E-04
500	3.55	1.0E+00	9.7E-01	8.7E-01	6.9E-01	4.7E-01	2.8E-01	1.5E-01	6.9E-02	2.9E-02	1.1E-02	3.7E-03	1.1E-03	3.3E-04
550	3.905	1.0E+00	9.8E-01	9.0E-01	7.5E-01	5.5E-01	3.5E-01	2.0E-01	1.0E-01	4.6E-02	6.9E-03	2.4E-03	7.5E-04	
600	4.26	1.0E+00	9.9E-01	9.3E-01	8.0E-01	6.2E-01	4.2E-01	2.6E-01	1.4E-01	6.8E-02	3.0E-02	1.2E-02	4.5E-03	1.5E-03
650	4.615	1.0E+00	9.9E-01	9.4E-01	8.4E-01	6.8E-01	4.9E-01	3.2E-01	1.8E-01	9.6E-02	4.6E-02	2.0E-02	8.0E-03	2.9E-03
700	4.97	1.0E+00	9.9E-01	9.6E-01	8.7E-01	7.3E-01	5.5E-01	3.8E-01	2.3E-01	1.3E-01	6.6E-02	3.1E-02	1.3E-02	5.2E-03
750	5.325	1.0E+00	1.0E+00	9.7E-01	9.0E-01	7.8E-01	6.1E-01	4.4E-01	2.9E-01	1.7E-01	9.1E-02	4.5E-02	2.1E-02	8.7E-03
800	5.68	1.0E+00	1.0E+00	9.8E-01	9.2E-01	8.2E-01	6.7E-01	5.0E-01	3.4E-01	2.1E-01	1.2E-01	6.4E-02	3.1E-02	1.4E-02
850	6.035	1.0E+00	1.0E+00	9.8E-01	9.4E-01	8.5E-01	7.2E-01	5.6E-01	4.0E-01	2.6E-01	1.6E-01	8.6E-02	4.4E-02	2.1E-02
900	6.39	1.0E+00	1.0E+00	9.9E-01	9.5E-01	8.8E-01	7.6E-01	6.1E-01	4.6E-01	3.1E-01	2.0E-01	1.1E-01	6.1E-02	3.0E-02
950	6.745	1.0E+00	1.0E+00	9.9E-01	9.6E-01	9.0E-01	8.0E-01	6.7E-01	5.1E-01	3.6E-01	2.4E-01	1.4E-01	8.1E-02	4.3E-02
1000	7.1	1.0E+00	1.0E+00	9.9E-01	9.7E-01	9.2E-01	8.4E-01	7.1E-01	5.7E-01	4.2E-01	2.8E-01	1.8E-01	1.1E-01	5.8E-02

**Table S5.** Determination of consensus site enrichment. This table shows the probability of observing a given number of Cdk1 consensus sites in a protein of a certain length, as determined by the Poisson distribution. p-values of less than 0.01 (indicated in red) were used to define enrichment of consensus sites in Fig. 4B.

Protein	<i>S. cerevisiae</i>	<i>C. albicans</i>	<i>S. pombe</i>	<i>X. laevis</i>	<i>H. sapiens</i>	References
Cdc6	X		X		X	21 - 25
Cdh1	X				X	26 - 28
Fkh2	X		X			29, 30
Iqq1		X				31
Mcm3	X				X	32, 33
Orc2	X		X			34, 35
Rga2	X	X				36, 37
Swe1	X		X	X	X	38 - 40

**Table S6.** Conservation of Cdk1 substrate regulation in other species. Previous studies provide examples of conserved biological function for shifting phosphorylation site clusters that we identified in the eight proteins listed in the left column. In many cases, conservation of regulation has persisted from *S. cerevisiae* to *Schizosaccharomyces pombe* or *Homo sapiens*. These proteins appear to be more predominantly regulated by plastic mechanisms than the general set of sites we identified (i.e. they exhibit significantly older site enrichment than the other 299 substrates [t-test p = 0.016] but not significantly older conservation of precise position [t-test p = 0.18]).

## References

1. A. C. Bishop *et al.*, *Nature* **407**, 395 (2000).
2. A. Gruhler *et al.*, *Mol Cell Proteomics* **4**, 310 (2005).
3. F. Stegmeier, R. Visintin, A. Amon, *Cell* **108**, 207 (2002).
4. F. Stegmeier, A. Amon, *Annu Rev Genet* **38**, 203 (2004).
5. S. A. Beausoleil, J. Villen, S. A. Gerber, J. Rush, S. P. Gygi, *Nat Biotechnol* **24**, 1285 (2006).
6. J. Villen, S. A. Beausoleil, S. A. Gerber, S. P. Gygi, *Proc Natl Acad Sci U S A* **104**, 1488 (2007).
7. J. Villen, S. P. Gygi, *Nat Protoc* **3**, 1630 (2008).
8. J. E. Elias, S. P. Gygi, *Nat Methods* **4**, 207 (2007).
9. C. E. Bakalarski *et al.*, *J Proteome Res* **7**, 4756 (2008).
10. E. Quevillon *et al.*, *Nucleic Acids Res* **33**, W116 (2005).
11. K. Shimizu, S. Hirose, T. Noguchi, *Bioinformatics* **23**, 2337 (2007).
12. D. T. Jones, *J Mol Biol* **292**, 195 (1999).
13. K. Peng, P. Radivojac, S. Vucetic, A. K. Dunker, Z. Obradovic, *BMC Bioinformatics* **7**, 208 (2006).
14. T. Ishida, K. Kinoshita, *Nucleic Acids Res* **35**, W460 (2007).
15. B. B. Tuch, D. J. Galgoczy, A. D. Hernday, H. Li, A. D. Johnson, *PLoS Biol* **6**, e38 (2008).
16. F. Chen, A. J. Mackey, C. J. Stoeckert, Jr., D. S. Roos, *Nucleic Acids Res* **34**, D363 (2006).
17. K. Kakiuchi *et al.*, *Biochemistry* **46**, 7781 (2007).
18. S. Ghaemmaghami *et al.*, *Nature* **425**, 737 (2003).
19. J. A. Ubersax *et al.*, *Nature* **425**, 859 (2003).
20. E. I. Boyle *et al.*, *Bioinformatics* **20**, 3710 (2004).
21. A. Calzada, M. Sanchez, E. Sanchez, A. Bueno, *J Biol Chem* **275**, 9734 (2000).
22. B. Baum, H. Nishitani, S. Yanow, P. Nurse, *EMBO J* **17**, 5689 (1998).
23. A. Lopez-Girona, O. Mondesert, J. Leatherwood, P. Russell, *Mol Biol Cell* **9**, 63 (1998).
24. V. Q. Nguyen, C. Co, J. J. Li, *Nature* **411**, 1068 (2001).

25. N. Mailand, J. F. Diffley, *Cell* **122**, 915 (2005).
26. W. Zachariae, M. Schwab, K. Nasmyth, W. Seufert, *Science* **282**, 1721 (1998).
27. S. L. Jaspersen, J. F. Charles, D. O. Morgan, *Curr. Biol.* **9**, 227 (1999).
28. E. R. Kramer, N. Scheuringer, A. V. Podtelejnikov, M. Mann, J. M. Peters, *Mol Biol Cell* **11**, 1555 (2000).
29. A. Pic-Taylor, Z. Darieva, B. A. Morgan, A. D. Sharrocks, *Mol Cell Biol* **24**, 10036 (2004).
30. M. Shimada *et al.*, *EMBO J* **27**, 132 (2008).
31. C. R. Li, Y. M. Wang, Y. Wang, *EMBO J* **27**, 2998 (2008).
32. V. Q. Nguyen, C. Co, K. Irie, J. J. Li, *Curr Biol* **10**, 195 (2000).
33. D. I. Lin, P. Aggarwal, J. A. Diehl, *Proc Natl Acad Sci U S A* **105**, 8079 (2008).
34. A. Vas, W. Mok, J. Leatherwood, *Mol Cell Biol* **21**, 5767 (2001).
35. D. Remus, M. Blanchette, D. C. Rio, M. R. Botchan, *J Biol Chem* **280**, 39740 (2005).
36. R. Sopko, D. Huang, J. C. Smith, D. Figeys, B. J. Andrews, *EMBO J* **26**, 4487 (2007).
37. X. D. Zheng, R. T. Lee, Y. M. Wang, Q. S. Lin, Y. Wang, *EMBO J* **26**, 3760 (2007).
38. S. Y. Kim, J. E. Ferrell, Jr., *Cell* **128**, 1133 (2007).
39. S. Y. Kim, E. J. Song, K. J. Lee, J. E. Ferrell, Jr., *Mol Cell Biol* **25**, 10580 (2005).
40. S. L. Harvey, A. Charlet, W. Haas, S. P. Gygi, D. R. Kellogg, *Cell* **122**, 407 (2005).

## Supporting databases (Excel spreadsheets)

**Database S1.** Complete list of phosphopeptides. Three separate quantitative (SILAC) experiments were performed to identify Cdk1 substrates by specific kinase inhibition (each is presented as a separate sheet): first, using a population of asynchronous cells (cdk1as\_asynchronous), second, using metaphase-arrested cells (cdk1as\_nocodazole), and third, using cells arrested in late mitosis by expression of a non-degradable truncated cyclin (cdk1as\_clb2). Usually twelve fractions for each experiment were analyzed in duplicate by LC-MS/MS (see details in each sheet). A total of 354,560 MS/MS spectra were collected. For database searching we used the Sequest algorithm against a composite target/decoy *S. cerevisiae* ORF protein sequence database, which allowed for the determination of a false-positive rate based on the number of reverse-sequence identifications in the final list. Sequest results were filtered based on criteria described in the Supplementary Methods section above. The final list contained 111,547 peptide spectral matches, of which 74,093 were phosphopeptides with 250 phosphopeptide reverse-sequence matches. The estimated false-discovery rate in phosphopeptide identification of the data set provided here (containing 73,843 phosphopeptides after removing reverse-hits) is 0.34%.

All MS/MS spectra successfully matching phosphopeptides are provided as active links. Phosphorylation sites are followed by the "\*" symbol, heavy-labeled lysines and arginines are denoted by "#" and "@" symbols, respectively, and oxidized methionines are denoted by the "^" symbol. An A-score value was calculated for each phosphorylation site on the peptide, and their values are listed from N to C terminus. Peptides with only one possibility of phosphorylation site(s) location did not require an A-score calculation and the Ascore\_1 column shows "1000". Those sites with A-score values > 13 were considered localized with >95% certainty; otherwise, they were called ambiguous, and the region in the peptide sequence where the phosphorylation can be localized is provided (columns region\_1, region\_2, region\_3; numbers denote distance from the residue where the phosphorylation has been arbitrarily placed). After removing redundancy from this list, 10,656 non-redundant phosphorylation sites were identified in 2,517 proteins. dCn' is defined here as the dCn value from the Sequest output file to the first peptide of different sequence (excluding modifications).

**Database S2.** High confidence phosphorylation sites from the three biological experiments. This list shows all unique phosphorylation sites that were identified with high confidence quantification (Vista score  $\geq$  86 and signal to noise S/N average  $\geq$  3) and  $>95\%$  confidence in the precise localization of the phosphorylation site (Ascore  $>$  13). The complete list of all phosphorylation sites is presented in the first sheet (all\_experiments). This table also shows the sequence context of the phosphorylated residue (centered\_15mer). Three columns (columns F-H: log<sub>2</sub>H/L\_asynchronous, log<sub>2</sub>H/L\_nocodazole, log<sub>2</sub>H/L\_clb2) provide the quantification of H/L ratios for every experiment in which that phosphorylation event was observed (note: when only the light or heavy peptide was observed, the signal to noise background level was used to define the ratio. These quantifications are denoted with < or > symbols). To remove redundancy from multiple peptides, we used the H/L value from the peptide with the best quantification (Vista score) and signal to noise (S/N average). Where phosphorylation events were observed in multiple high confidence peptides, we used the H/L value from the peptide with the least number of non-(S/T)\*-P phosphorylation sites to minimize the number of false positives in our Cdk1-dependent dataset (i.e. phosphopeptides whose abundance change could possibly be assigned to other dynamic phosphorylation events). This database includes a small number of peptides phosphorylated on tyrosine and a small number of sites that fail to align perfectly with the yeast genome S288C sequence; these sites were not included in the analysis in Figure 1 or other figures.

The subsequent sheets contain lists of the precise peptide sequences obtained in each of the three experiments (as described above) - asynchronous cells (asynchronous), metaphase-arrested cells (nocodazole), and cells arrested in late mitosis (clb2).